More about the Wilsonian analysis on the pionless NEFT

Koji Harada,[*] Hirofumi Kubo,[†] and Atsushi Ninomiya[‡]

Department of Physics, Kyushu University

Fukuoka 812-8581 Japan

(Dated: July 30, 2009)

Abstract

We extend our Wilsonian renormalization group (RG) analysis on the pionless nuclear effective theory (NEFT) in the two-nucleon sector in two ways; on the one hand, (1) we enlarge the space of operators up to including those of $\mathcal{O}(p^4)$ in the S waves, and, on the other hand, (2) we consider the RG flows in higher partial waves (P and D waves). In the larger space calculations, we find, in addition to nontrivial fixed points, two "fixed lines" and a "fixed surface" which are related to marginal operators. In the higher partial wave calculations, we find similar phase structures to that of the S waves, but there are *two* relevant directions in the P waves at the nontrivial fixed points and *three* in the D waves. We explain the physical meaning of the P-wave phase structure by explicitly calculating the low-energy scattering amplitude. We also discuss the relation between the Legendre flow equation which we employ and the RG equation by Birse, McGovern, and Richardson, and possible implementation of Power Divergence Subtraction (PDS) in higher partial waves.

[*]Electronic address: harada@phys.kyushu-u.ac.jp

[†]Electronic address: kubo@higgs.phys.kyushu-u.ac.jp

[‡]Electronic address: ninomiya@higgs.phys.kyushu-u.ac.jp

I. INTRODUCTION

Nuclear effective field theory (NEFT) [1, 2, 3] is a low-energy effective field theory of nucleons based on the general principles of quantum field theory and the symmetries of the underlying theory of hadrons, QCD. (See Ref. [4, 5, 6] for reviews.) At very low energies, where even the pions are regarded as "heavy," interactions of nonrelativistic nucleons are simulated by (infinitely many) contact operators. Such a theory is called *pionless* NEFT with the physical cutoff scale being around the pion mass, while the *pionful* NEFT is needed at higher energies, where the effects of the exchange of pions are explicitly taken into account. Because NEFT contains infinitely many operators, one needs an organizing principle, called power counting, to systematically calculate physical quantities to a certain order.

It is interesting to note that the actual two-nucleon system in the S waves is fine-tuned. The scattering lengths are unnaturally large compared to the scale characteristic to the two-nucleon interaction. From the RG point of view, this unnaturalness may be rephrased as that the system is very close to the nontrivial fixed point (or better, to the critical surface) [7, 8]. The two-nucleon system is thus nonperturbative due not only to the strong coupling, but also to the closeness to the critical surface.

The unnaturalness of NEFT makes the power counting issue complicated. The so-called Naive Dimensional Analysis (NDA) [9] works for perturbative systems, but does not account for fine-tuning. One needs a power counting which encodes the fine-tuning. There are a lot of papers [7, 8, 10, 11, 12, 13, 14, 15, 16, 17] devoted to the power counting issues in NEFT, and it is still an important subject of discussions.

In a previous paper [18], two of the present authors performed a Wilsonian RG analysis [19, 20, 21, 22] of pionless NEFT to determine the power counting of the operators in the $^1S_0$ and $^3S_1$-$^3D_1$ channels on the basis of the scaling dimensions at the nontrivial fixed point. We employed the Legendre flow equation [23, 24, 25, 26, 27] as a formulation of nonperturbative RG, and we reproduced known results obtained by Birse et al. [28] up to $\mathcal{O}(p^2)$ in a completely field theoretical fashion. We also emphasized the phase structure and identified the inverse of the scattering length as the order parameter. In the *strong coupling phase*, there is a coupling which grows as the floating cutoff Λ is lowered, and there is a bound state, while in the *weak coupling phase*, all the flows run into the trivial fixed point and there is no bound state. The determination of the power counting on the basis of the

scaling dimensions is a unifying principle of EFT, useful especially for the cases in which nonperturbative dynamics is important.

One of the good features of Wilsonian RG analysis of EFT is that it provides an overview of all the possible theories consistent with the symmetries, not restricted only to the one that describes the real world. In other words, it characterizes the physical system in a broad perspective in terms of the RG flows.

Although the formulation of the Legendre flow equation does not contain any approximation, in order to solve it, one needs an approximation; the restriction of the space of operators. It is important to note that the restriction does not require an *a priori* power counting more than just the canonical dimensional counting. The point is to include a sufficient number of operators. The scaling dimensions are determined for the linear combinations of the operators included at each fixed point.

It is important to note that when the space of operators is enlarged, the results (e.g., the scaling dimensions) are expected to always converge to the true values. The question is *how fast* they converge. In order to see it, it is necessary to actually enlarge the space of operators. If the enlargement does not alter the results of the calculations with smaller space very much, we may conclude that the results are close to the true values. It has been argued that the small dependence on the choice of cutoff functions also suggests fast convergence [29].

Since our formulation is quite general, we can readily do a similar analysis to other systems. For example, one can investigate higher partial waves, where higher derivative terms play an important role. Note however that, in general, higher partial waves are physically not so significant at very low energies and that the physical two-nucleon system does not seem to be fine-tuned in those higher partial waves. Nevertheless, it is interesting to perform the RG analysis for higher partial waves, because it provides a better characterization of the physical two-nucleon systems than just that of the angular momentum. (How many nontrivial fixed points there are? How far is the physical system from them?) This kind of information may be useful in the study of other systems described by a similar EFT.

One may think of the so-called "halo nuclei" as such an example. A typical halo nucleus consists of a core (e.g., alpha-particle) and a few "halo" nucleons, and an EFT is proposed to describe such a system [30]. A particularly interesting example is the nucleon-alpha scattering in the P-wave, for which the $p_{3/2}$ channel displays a resonance just above the

threshold [30, 31]. Such a resonance is clearly related to a RG critical surface. The RG structure for nucleon-alpha scattering is very similar to that of the pionless NN scattering, which we consider in this paper. We provide an account on the power counting of Refs. [30, 31] on the basis of Wilsonian RG analysis

In this paper, we continue our previous study and perform a Wilsonian RG analysis of pionless NEFT in two-nucleon sector. After recapitulating the previous paper, we first enlarge the space of operators to include those of $\mathcal{O}(p^4)$ in the $^1S_0$ channel. We find two "fixed lines" and a "fixed surface" besides trivial and nontrivial fixed points. The nontrivial fixed point that we think the most relevant to the real world persists, and the scaling dimensions of the eigen-operators of the linearized RGE do not change, consistent with Ref. [28].

Second, we consider the P waves and obtain the phase structure by solving the RG equations. The phase structure is similar to that in the S waves, but there are *two* relevant operators in the P waves at the nontrivial fixed points. We also discuss briefly the D waves and find that there are *three* relevant ones.

The structure of the paper is the following: In Sec. II we recapitulate the main points of the previous paper [18] in order to introduce the notations and the main concepts in our analysis. Since the present paper closely follows the discussions given in Ref. [18], we expect that the readers intimately consult with Ref. [18]. In Sec. III we discuss the enlargement of the space of operators. The calculations for the higher partial waves are given in Sec. IV. We also discuss possible extensions of Power Divergence Subtraction (PDS) renormalization for higher partial waves. The summary and discussions are given in Sec. V. In Appendix A, we discuss the relation between the Legendre flow equation in the sharp cutoff limit and the RG equation used by Birse et al. [28]. The cutoff function dependence of the results is studied in Appendix B.

II. NONPERTURBATIVE RG ANALYSIS FOR THE TWO-NUCLEON SYSTEM AT VERY LOW ENERGIES

A. Power counting and the scaling dimensions

The most basic idea behind the power counting is the order of magnitude estimate based on dimensional analysis. For the two-nucleon system at very low energies described by the

pionless NEFT, there is a physical cutoff scale $\Lambda_0 \sim \mathcal{O}(m_\pi)$, above which the effective theory is not applicable. Since it is the only scale (except for the nucleon mass, M, see the footnote 3 of Ref. [18] and the section 1.2.1 of Ref. [32]) which appears in the pionless NEFT, the dimensional analysis for the pionless NEFT is based on this scale.

Quantum fluctuations may change the classical dimensional analysis. The quantum counter part of the dimension is the *scaling dimension*, which can be obtained by the RG analysis. It is therefore natural to consider the power counting based on the scaling dimensions. Wilsonian, or nonperturbative, RG is a suitable tool to handle the quantum fluctuations.

It is known that there is another scale in the two-nucleon system, the scattering length in an S wave, the inverse of which is much smaller than Λ_0. It can be understood that such a scale is not fundamental, but is a result of the fine-tuning of the parameters of the EFT. In the RG language, the fine-tuning is closely related to the existence of a nontrivial fixed point and a critical surface of the RGE. It has been shown that on the critical surface the scattering length is infinite. In order to get a large scattering length, the coupling constants must be fine-tuned to be near the critical surface.

Around the nontrivial fixed points the scaling dimensions are drastically different from their classical values, the canonical dimensions. The coupling which corresponds to the scattering length classically has negative dimension, indicating that it gets less important at lower energies. But near the nontrivial fixed point (or the critical surface), the (quantum) scaling dimension is positive, so the corresponding interaction becomes more important at lower energies. On the other hand, near the trivial fixed point, where all the coupling constants are small, the scaling dimensions are the same as the classical values. There the quantum fluctuations do not alter the importance of the interaction.

A relevant operator, which has a positive scaling dimension, controls the deviation of the coupling constants from a critical surface. In order to get a scale much smaller than Λ_0, the relevant operator must be fine-tuned. Near a nontrivial fixed point, the number of the parameters to be fine-tuned is that of the relevant operators.

In determining the *power counting*, one usually does two things: (1) choose a set of operators one is going to work with, and (2) determine the importance of the operators. In a conventional power counting scheme, one first determines the importance of the operators (2) by assuming some scaling property, and it then leads to the set of operators (1) to

a given order. On the other hand, in the Wilsonian RG approach we only choose a set of operators (1). The importance of the operators (2) is determined as an output by the scaling dimensions of them.

In most cases, it is unlikely to miss important operators in both approaches, as far as one includes all the operators of low canonical dimensions to a certain order. What matters is the determination of the importance of the operators (the scaling property).

Up to the point where the fixed points and the scaling dimensions are obtained in the Wilsonian RG approach, however, no contact has been made with where the real world is in the RG flow. The Wilsonian RG approach reveals all the possible theories described by the same action without the knowledge of the actual systems. It is the strength as well as the weakness of the approach. Namely, one can determine possible scaling properties consistent with the action (the symmetry, spacetime dimensions, and the degrees of freedom) while one still needs additional information about the system (e.g., a large scattering length) one is trying to describe, in order to determine where it is in the RG flow.

Convergence of the approximation has different meanings in the conventional and the Wilsonian RG approaches: in the conventional approach, the validity of the power counting is examined (in most cases, numerically) *whether* the expansion converges. With a wrong assumption of scaling property, the expansion fails to converge, i.e., even though one includes more operators, the results (the phase shift of a specific channel, for example) do not improve. See Ref. [13] for the important example. On the other hand, in the Wilsonian RG approach, the results (the scaling dimensions at a specific fixed point, for example) improve as the space of the operators is enlarged. The question is *how fast* the results converge.

B. Legendre flow equation

Legendre flow equation [23, 24, 25, 26, 27] is one of the implementations of Wilsonian RGE. It is formulated as a RGE for the infrared (IR) cutoff effective action $\Gamma_\Lambda[\Phi]$ called *effective averaged action*, in which the quantum fluctuations above the cutoff have been integrated. The averaged action is the generator of the one-particle irreducible (1PI) vertex functions containing only the fluctuations $p \gtrsim \Lambda$.

The Legendre flow equation is given by

$$\frac{d\Gamma_\Lambda}{d\Lambda} = \frac{i}{2}\text{Tr}\left[\frac{dR_\Lambda}{d\Lambda}\left(\Gamma_{(2)} + R_\Lambda\right)^{-1}\right], \tag{2.1}$$

where $\Gamma_{(2)}$ stands for the second derivative of the averaged action Γ_Λ with respect to the fields, and is the inverse of the full propagator dressed by the vertices with classical field insertions, containing only the fluctuations $p \gtrsim \Lambda$, and the Tr denotes the integration over momentum and also the trace in the internal space. The function R_Λ effectively cuts off the IR part of the fluctuations. Our choice is, as in the previous paper, as follows;

$$R_\Lambda(\boldsymbol{p}^2) = \frac{\boldsymbol{p}^2}{2M}\left[1 - \exp\left[\left(\frac{\boldsymbol{p}^2}{\Lambda^2}\right)^n\right]\right]^{-1}, \tag{2.2}$$

where $\boldsymbol{p}$ is the three-momentum. In the $n \to \infty$ limit, it becomes a sharp cutoff. Another choice is adopted in Ref. [33]. We derive the RGE for an arbitrary value of n, but the results look so complicated that we present only the results in the $n \to \infty$ limit. The n-dependence is studied in Appendix B.

In the application to the two-nucleon system, we have drastic simplification of the RGE. (i) Because of the nonrelativistic feature of the system, we do not include anti-particles. Thus there are no self-energy corrections, nor tadpole contributions. (ii) In the two-nucleon sector only the four-nucleon (4N) operators contribute. From these, we end up with the one-loop diagrams involving two vertices with the tree-level propagators contributing to the Legendre flow equation. The multi-loop effects are encoded in the cutoff dependence of the (infinitely many) coupling constants.

In Appendix A, we discuss the relation between the Legendre flow equation in the sharp cutoff limit and the RG equation used by Birse et al. for the potential V,

$$\frac{\partial V}{\partial \Lambda} = \frac{M}{2\pi^2}V(k', \Lambda, p; \Lambda)\frac{\Lambda^2}{\Lambda^2 - p^2}V(\Lambda, k, p; \Lambda). \tag{2.3}$$

(See Ref. [28] for details.) It is shown that they are essentially equivalent.

As we emphasized in Ref. [18], there is no obvious way of imposing a Galilean invariant cutoff at the averaged action level [33], so that the inclusion of the IR cutoff function in the averaged action should be understood as a symbolic one. Note that the IR cutoff function constrains the momenta of individual particles, but they are not invariants under Galilean transformations. Fortunately, however, the correct way of implementing a cutoff is clear in the two-nucleon system; to impose the cutoff on the relative three momentum. See Sec. 4.1

in Ref. [18] for the explicit manipulation. Note that it is *not* an approximation, but the *only* way that we know to implement the cutoff in a Galilean invariant way.

C.   Pionless NEFT up to $\mathcal{O}(p^2)$ in the $^1S_0$ channel

Although the Legendre flow equation is *exact*, one needs an approximation to solve it. We consider a simple truncation of the space of operators. We retain only the operators with derivatives up to a certain order. We simply count the number of spatial derivatives ($\nabla \sim p$) and a time derivative is counted as two spatial derivatives ($\partial_t \sim p^2$). The approximation is based on our hope that, even though some operators get large anomalous dimensions, their "ordering" of importance would not change very much; the lower the canonical dimension is, the lower the scaling dimension would be. We also expect that there are mixings among operators. In Ref. [18], we consider the following ansatz for the averaged action up to $\mathcal{O}(p^2)$,

$$\Gamma_\Lambda^{(p^2)} = \int d^4x \left[N^\dagger \left(i\partial_t + \frac{\nabla^2}{2M} \right) N - C_0 \left(N^T P_a^{(^1S_0)} N \right)^\dagger \left(N^T P_a^{(^1S_0)} N \right) \right.$$
$$+ C_2 \left[\left(N^T P_a^{(^1S_0)} N \right)^\dagger \left(N^T P_a^{(^1S_0)} \overleftrightarrow{\nabla}^2 N \right) + \text{h.c.} \right]$$
$$\left. + 2B \left[\left\{ N^T P_a^{(^1S_0)} \left(i\partial_t + \frac{\nabla^2}{2M} \right) N \right\}^\dagger \left(N^T P_a^{(^1S_0)} N \right) + \text{h.c.} \right] \right], \qquad (2.4)$$

for the $^1S_0$ channel, where $P_a^{(^1S_0)}$ is the projection operator to the channel,

$$P_a^{(^1S_0)} = \frac{1}{\sqrt{8}} \sigma^2 \tau^2 \tau^a, \qquad (2.5)$$

and $\overleftrightarrow{\nabla}^2 \equiv \overleftarrow{\nabla^2} + \overrightarrow{\nabla^2} - 2\overleftarrow{\nabla} \cdot \overrightarrow{\nabla}$. As we emphasized in a previous paper [34], it is important to include the so-called "redundant operators," which can be eliminated from the action by using the equations of motion.

By introducing the following dimensionless coupling constants,

$$x = \frac{M\Lambda}{2\pi^2} C_0, \quad y = \frac{M\Lambda^3}{2\pi^2} 4C_2, \quad z = \frac{\Lambda^3}{2\pi^2} B, \qquad (2.6)$$

8

the RGEs can be expressed as

$$\frac{dx}{dt} = -x - \left[x^2 + 2xy + y^2 + 2xz + 2yz + z^2 \right], \tag{2.7}$$

$$\frac{dy}{dt} = -3y - \left[\frac{1}{2}x^2 + 2xy + \frac{3}{2}y^2 + yz - \frac{1}{2}z^2 \right], \tag{2.8}$$

$$\frac{dz}{dt} = -3z + \left[\frac{1}{2}x^2 + xy + \frac{1}{2}y^2 - xz - yz - \frac{3}{2}z^2 \right], \tag{2.9}$$

where $t = \ln(\Lambda_0/\Lambda)$. We found a nontrivial fixed point,

$$(x^\star, y^\star, z^\star) = \left(-1, -\frac{1}{2}, \frac{1}{2} \right), \tag{2.10}$$

as well as the trivial one $(0, 0, 0)$. The eigenvalues and the corresponding eigenvectors of the linearized RGE at the nontrivial fixed points are found to be

$$\nu_1 = +1: \quad \boldsymbol{u}_1 = (1, 1, -1), \tag{2.11}$$

$$\nu_2 = -1: \quad \boldsymbol{u}_2 = (0, -1, 1), \tag{2.12}$$

$$\nu_3 = -2: \quad \boldsymbol{u}_3 = (2, -1, -2). \tag{2.13}$$

(Note that the signs and the normalizations of the eigenvectors are arbitrary.) The eigenvector associated with the positive eigenvalue ν_1 corresponds to the scattering length.

In Ref. [34] we performed a similar RG analysis based on the cutoff independence of the amplitude and found the same scaling dimensions with slightly different eigenvectors. Since eigenvectors are not universal quantities and the approximations are different, it is therefore not surprising that the eigenvectors are different. The important thing is that the eigenvalues, which are considered as the universal ones, actually agree. The fact that the first two eigenvectors agree reflects that these two approximations are similar.

These results are obtained with a severe restriction of the space of operators. One should examine the validity of the approximation by actually enlarging the space of operators. It is expected that some properties, i.e., the scaling dimensions at the nontrivial fixed points, are universal and would not change very much under the enlargement if the approximation is good, while the others such as the directions of eigenvectors may change. It is well known that the restriction of the space of operators causes various artefacts [35, 36, 37].

In the next Section, we investigate the effects of the enlargement of the space of operators and compare the results with the previous ones presented in this section.

III. PIONLESS NEFT UP TO $\mathcal{O}(p^4)$ IN THE $^1S_0$ CHANNEL

A. Independent operators

In this section, we enlarge the space of operators in the $^1S_0$ channel up to including those of $\mathcal{O}(p^4)$. (The results for the $^3S_1$-$^3D_1$ channel are essentially the same as those for the $^1S_0$, but a bit more complicated.) We consider the following ansatz for the averaged action,

$$
\begin{aligned}
\Gamma^{(p^4)}_\Lambda = \Gamma^{(p^2)}_\Lambda \\
+ \int d^4x \Bigg[&- C_{41} \left[\left(N^T P_a^{(^1S_0)} N \right)^\dagger \left(N^T P_a^{(^1S_0)} \overleftrightarrow{\nabla}^4 N \right) + \text{h.c.} \right] \\
&- C_{42} \left(N^T P_a^{(^1S_0)} \overleftrightarrow{\nabla}^2 N \right)^\dagger \left(N^T P_a^{(^1S_0)} \overleftrightarrow{\nabla}^2 N \right) \\
&+ 2B_1 \left[\left(N^T P_a^{(^1S_0)} N \right)^\dagger \left\{ N^T P_a^{(^1S_0)} \left(i\partial_t + \frac{\nabla^2}{2M} \right)^2 N \right\} + \text{h.c.} \right] \\
&+ 4B_2 \left\{ N^T P_a^{(^1S_0)} \left(i\partial_t + \frac{\nabla^2}{2M} \right) N \right\}^\dagger \left\{ N^T P_a^{(^1S_0)} \left(i\partial_t + \frac{\nabla^2}{2M} \right) N \right\} \\
&- 2B_3 \left[\left(N^T P_a^{(^1S_0)} \overleftrightarrow{\nabla}^2 N \right)^\dagger \left\{ N^T P_a^{(^1S_0)} \left(i\partial_t + \frac{\nabla^2}{2M} \right) N \right\} + \text{h.c.} \right] \Bigg]. \quad (3.1)
\end{aligned}
$$

We emphasize that the ansatz given above contains all the independent operators consistent with Galilean invariance, parity, spin and isospin invariance to the given order. There are actually two other operators which satisfies these requirements,

$$
\left[\left(N^T P_a^{(^1S_0)} N \right)^\dagger \left\{ N^T P_a^{(^1S_0)} \overleftrightarrow{\nabla}^2 \left(i\partial_t + \frac{\nabla^2}{2M} \right) N \right\} + \text{h.c.} \right], \quad (3.2)
$$

$$
\left[\left(N^T P_a^{(^1S_0)} N \right)^\dagger \left\{ N^T P_a^{(^1S_0)} \left(i\overleftarrow{\partial}_t + \frac{\overleftarrow{\nabla}^2}{2M} \right) \left(i\partial_t + \frac{\nabla^2}{2M} \right) N \right\} + \text{h.c.} \right], \quad (3.3)
$$

but they are written as linear combinations of the operators contained in the averaged action up to total derivatives, and thus we dropped them. The relations may be expressed most clearly in momentum space. Using momentum conservation, $(p_1 + p_2)^\mu = (p_3 + p_4)^\mu$, we

obtain

$$r_{12}\left(S_1 + S_2\right) + r_{34}\left(S_3 + S_4\right) = r_{12}\left(S_1 + S_4\right) + r_{34}\left(S_1 + S_2\right)$$
$$- \frac{1}{4M}\left(r_{12}^2 + r_{34}^2\right) + \frac{1}{2M}r_{12}r_{34}, \tag{3.4}$$

$$S_1 S_2 + S_3 S_4 = \left(S_1 + S_2\right)\left(S_3 + S_4\right) - \frac{1}{2}\sum_{i=1}^4 S_i$$
$$+ \frac{1}{32M}\left(r_{12}^2 + r_{34}^2\right) - \frac{1}{16M}r_{12}r_{34}, \tag{3.5}$$

where we have introduced the notations,

$$r_{ij} \equiv \left(\boldsymbol{p}_i - \boldsymbol{p}_j\right)^2, \quad S_i \equiv p_i^0 - \frac{\boldsymbol{p}_i^2}{2M}. \tag{3.6}$$

It is also important to note that we have included the interaction (B_1) which depends not only on the total energy of the two nucleons, but on the individual energies. The potential corresponding to this interaction is not considered in Ref. [28].

We do not include the relativistic correction terms such as $N^\dagger\left(\nabla^4/8M^3\right)N$ in the averaged action because it breaks Galilean invariance. It means that we are considering the system at very low energies so that the relativistic corrections can be neglected. The effect of this term is estimated to be smaller than any of the terms we have included in Eq. (3.1) due to the additional $\mathcal{O}\left((\Lambda/M)^2\right)$ suppression.

B.   RG equations

The Legendre flow equation may be obtained in a similar manner as in Ref. [18], which generalizes the set of RGEs (2.7), (2.8), and (2.9).

By introducing the following dimensionless coupling constants,

$$u_i = \frac{M\Lambda^5}{2\pi^2}16C_{4i}\ (i=1,2), \quad z_i = \frac{\Lambda^5}{2\pi^2 M}B_i\ (i=1,2), \quad z_3 = \frac{\Lambda^5}{2\pi^2}4B_3, \tag{3.7}$$

together with x, y, and z defined in (2.6), we have a set of the RGEs for these variables in

the $n \to \infty$ limit,

$$
\begin{aligned}
\frac{dx}{dt} = & - x - x(x + 2y + 2z + 2u_1 - 2z_1) - y(y + 2z + 2u_1 - 2z_1) \\
& - z(z + 2u_1 - 2z_1) - u_1(u_1 - 2z_1) - z_1^2,
\end{aligned} \tag{3.8}
$$

$$
\begin{aligned}
\frac{dy}{dt} = & - 3y - x \left(\frac{1}{2}x + 2y + u_1 + u_2 + z_1 + z_3 \right) - y \left(\frac{3}{2}y + z + 2u_1 + u_2 + z_3 \right) \\
& + z \left(\frac{1}{2}z - u_2 - 2z_1 - z_3 \right) - u_1 \left(\frac{1}{2}u_1 + u_2 + z_1 + z_3 \right) + u_2 z_1 \\
& + z_1 \left(\frac{3}{2}z_1 + z_3 \right),
\end{aligned} \tag{3.9}
$$

$$
\begin{aligned}
\frac{dz}{dt} = & - 3z + x \left(\frac{1}{2}x + y - z + u_1 + z_1 + z_2 - z_3 \right) + y \left(\frac{1}{2}y - z + u_1 + z_1 + z_2 - z_3 \right) \\
& - z \left(\frac{3}{2}z + u_1 - 3z_1 - z_2 + z_3 \right) + u_1 \left(\frac{1}{2}u_1 + z_1 + z_2 - z_3 \right) \\
& - z_1 \left(\frac{3}{2}z_1 + z_2 - z_3 \right),
\end{aligned} \tag{3.10}
$$

$$
\frac{du_1}{dt} = - 5u_1 - u_1(x + y + z + u_1 - z_1), \tag{3.11}
$$

$$
\begin{aligned}
\frac{du_2}{dt} = & - 5u_2 - x(x + 4y + 2u_1 + 2u_2) - y(4y + 4u_1 + 4u_2 + 2z_1 + 2z_3) + z(2z_1 + 2z_3) \\
& - u_1(u_1 + 2u_2) - u_2(u_2 + 2z_1 + 2z_3) - z_1(3z_1 + 4z_3) - z_3^2,
\end{aligned} \tag{3.12}
$$

$$
\frac{dz_1}{dt} = - 5z_1 - z_1(x + y + z + u_1 - z_1), \tag{3.13}
$$

$$
\begin{aligned}
\frac{dz_2}{dt} = & - 5z_2 + x(x + 2y - 2z + 2u_1 - 2z_3) + y(y - 2z + 2u_1 - 2z_3) \\
& + z(z - 2u_1 - 4z_1 - 4z_2 + 2z_3) + u_1(u_1 - 2z_3) + z_1(3z_1 + 4z_2 - 2z_3) \\
& + z_2(z_2 - 2z_3) + z_3^2,
\end{aligned} \tag{3.14}
$$

$$
\begin{aligned}
\frac{dz_3}{dt} = & - 5z_3 + x(x + 3y - z + 2u_1 + u_2 - z_3) + y(2y - 2z + 3u_1 + u_2 + z_1 + z_2 - 2z_3) \\
& - z(u_1 + u_2 + 3z_1 + z_2 + 2z_3) + u_1(u_1 + u_2 - z_3) + u_2(z_1 + z_2 - z_3) \\
& + z_1(3z_1 + 2z_2 + z_3) + z_2 z_3 - z_3^2.
\end{aligned} \tag{3.15}
$$

By setting $u_1 = u_2 = z_1 = z_2 = z_3 = 0$ by hand in the first three of these RGEs and ignoring the rest, they reduce to the ones, (2.7), (2.8), and (2.9), as they should. This is exactly what we did in the $\mathcal{O}(p^2)$ calculations.

To analyze the RG flows, it is useful to determine the fixed points, at which the coupling constants do not run. We use *Mathematica* to solve the fixed point equations and found the following solutions.

A $(0, 0, 0, 0, 0, 0, 0, 0)$,

B $\left(-1, -\frac{1}{2}, \frac{1}{2}, 0, -\frac{4}{3}, 0, \frac{4}{3}, \frac{4}{3}\right)$,

C $\left(-\frac{9}{4}, \frac{123}{44}, \frac{21}{22}, 0, -\frac{92889}{15488}, 0, \frac{13689}{15488}, -\frac{33831}{15488}\right)$,

D $\left(-25, \frac{175}{18}, -\frac{25}{6}, u_1, 20 - 2u_1, \frac{-130 + 9u_1}{9}, \frac{260 - 18u_1}{9}, \frac{10}{3}\right)$,

E $\left(0, 0, 0, 0, u_2, 0, X_\pm, \frac{-5X_\pm + X_\pm^2 + 5u_2 + 2X_\pm u_2 + u_2{}^2}{10}\right)$,

F $\left(-25, y, -y, u_1, \frac{23125 - 1000u_1 - 1700y + 36y^2}{500}, -20 + u_1, \frac{19375 - 1000u_1 + 300y - 36y^2}{500}, \frac{-1875 + 1000y - 36y^2}{500}\right)$,

where we have introduced

$$X_\pm = 5 \pm 2\sqrt{5}\sqrt{-u_2} - u_2. \tag{3.16}$$

The first fixed point [A] is the trivial fixed point. The second one [B] corresponds to the fixed point we considered in the previous paper (the fixed point Eq. (2.10)) because their first three coordinates coincide with each other. Note that, since the restriction of the space is nothing but the projection to the lower dimensional subspace, the fixed point Eq. (2.10) has the components which we naturally expect the corresponding fixed point to have if the approximation is good. As we explained in Ref. [18], this fixed point is the most relevant to the real two-nucleon systems, and we will discuss it later in detail. The third one [C] is a strange fixed point. We calculate the scaling dimensions at this point, and found that they are: $-8, -13/2, -13/2, 5, 3, 1$, and $(-5 \pm i\sqrt{41})/2$. Because of the appearance of the complex scaling dimensions, we suspect that this is an artefact of the truncation. We will give the argument shortly.

The fourth [D] and the fifth [E] are actually "fixed lines." The [D] is a fixed point for an arbitrary u_1, and the [E] for an arbitrary $u_2 \leq 0$. The [D] is a straight line, while the [E] is a parabolic curve with the peak at $(0, 0, 0, 0, 0, 0, 5, 0)$. The sixth [F] is an even stranger "fixed surface." Interestingly the scaling dimensions are the same on the whole fixed lines (surface). The scaling dimensions at [D] are: $5, 0, (11 \pm i\sqrt{239})/6, -7.86665 \pm 3.58098i$, and $-1.35557 \pm 0.309653i$. Since this also has complex scaling dimensions, we suspect that it is an artefact too. See below. The [E] has the scaling dimensions, $-5, -5, -5, -3, -1, 0, 2, 5$. Note that all the scaling dimensions are integers, and the existence of a marginal direction. Actually, a fixed point on it has been noticed by Birse [56]. The [F] has the scaling dimensions,

$-5, (-11 \pm \sqrt{41})/2, 0, 0, 2, 5, 7$. Note that there are two marginal directions, which are tangential to the surface.

We consider the fixed point [C] and and the fixed line [D], which have complex scaling dimensions, artefacts of the truncation. In the following, we argue for this statement by giving a list of observations. We admit that each of them is not completely convincing, but they all suggest that fixed objects with complex scaling dimensions are artefacts. Of course, there is no definite criterion by which we can decide whether a fixed object is an artefact.

The observations are the followings: (1) It is well known that the truncation generates complex scaling dimensions [36], and it seems a general feature of truncation. So the appearance of complex scaling dimensions can be seen as a signal of the artefact of the truncation and does not seem to have real physical relevance, at least in most cases. (2) In the literature, it is extremely rare for complex scaling dimensions that do not seem to be artefacts to appear in physical systems. To our best knowledge, only hierarchical Ising models [38] and gravitational collapse [39, 40] are such systems. The former are frustrated at every length scale, while the latter is known to have critical limit cycle (discrete self-similarity). We see that these examples are very different from the simple system of self-interacting nonrelativistic fermions. (3) In a previous paper [18] we found a fixed point with complex scaling dimensions, but when enlarging the space of operators in the present paper, we do not find the corresponding fixed point. It disappears. This is a concrete example of a nontrivial fixed point which appears with complex scaling dimensions in smaller space of operators, and is in fact an artefact of the truncation. It is important to note that the very existence of a nontrivial fixed point can be an artefact. (4) It seems unlikely to get complex scaling dimensions by the method employed by Birse *et al.* [28], which is proved in Appendix A to be essentially equivalent to ours. Note that, even though the RGE for the potential to be solved is shown to be the same for the both approaches, the way of solving it is different. In the approach by Birse *et al.* the scaling dimensions are the sums of the powers of the monomial perturbation around the (inverse of the) fixed point potential that is not expanded in powers of the energy. The scaling dimensions obtained in such a way should be integers. (5) Because of the nonrelativistic feature of the present theory, only power divergences are involved. It is therefore natural to expect integer scaling dimensions. From this point of view, the fractional scaling dimensions of the fixed surface [F] also seem to be artefacts.

Again, we cannot completely exclude the logical possibility that the fixed objects persist

in further enlargement of space of operators, while their scaling dimensions become real.

Even though their physical relevance is unclear at this moment, it is interesting to find such possibilities of several kinds of fixed objects appear in the system. These possibilities have never been revealed in other papers. Compare with the work by Birse et al. [28], for example. They started with an ansatz for a fixed potential that depends only on the total energy, found the solution, and analyzed perturbations around it. In our analysis, on the other hand, we scanned the whole (though restricted) theory space and found all possible fixed objects.

In any case, irrespective to whether these fixed objects are artefacts or not, the most relevant fixed point to the realistic two-nucleon systems is the fixed point [B]. It is easy to see that our solution is the same as the one obtained by Birse et al. [28] up to including $\mathcal{O}(p^4)$.

At the nontrivial fixed point [B], we find the following scaling dimensions and corresponding eigenvectors,

$$\nu_1 = +1: \quad \boldsymbol{u}_1 = \left(1, 1, -1, 0, \frac{11}{3}, 0, -\frac{11}{3}, -\frac{11}{3}\right), \tag{3.17}$$

$$\nu_2 = -1: \quad \boldsymbol{u}_2 = (0, -1, 1, 0, -4, 0, 4, 4), \tag{3.18}$$

$$\nu_3 = -2: \quad \boldsymbol{u}_3 = \left(1, 1, -\frac{5}{2}, 0, \frac{23}{3}, 0, -\frac{32}{3}, -\frac{55}{6}\right), \tag{3.19}$$

$$\nu_4 = -3: \quad \boldsymbol{u}_4 = (0, 0, 0, 0, 1, 0, -1, -1), \tag{3.20}$$

$$\nu_5 = -4: \quad \boldsymbol{u}_5 = \left(1, -1, 1, \frac{1}{2}, 0, 3, 0, 0\right), \tag{3.21}$$

$$\nu_6 = -4: \quad \boldsymbol{u}_6 = \left(1, -1, 1, -\frac{5}{2}, 6, 0, 6, 0\right), \tag{3.22}$$

$$\nu_7 = -4: \quad \boldsymbol{u}_7 = (-2, -1, 1, 5, -6, 0, 0, 3), \tag{3.23}$$

$$\nu_8 = -5: \quad \boldsymbol{u}_8 = \left(-\frac{1}{2}, -\frac{1}{2}, 2, 0, \frac{1}{6}, 0, \frac{22}{3}, \frac{4}{3}\right). \tag{3.24}$$

Note that (i) all the scaling dimensions are integers. (ii) The first three eigenvalues coincide with those obtained in the previous paper, which justifies the identification of the fixed point [B] in the present paper with the fixed point Eq. (2.10) in the previous paper. (iii) The results are insensitive to the choice of the cutoff function. We give the analysis of the n-dependence in Appendix B. (iv) Only the eigenvector $\boldsymbol{u}_5$ contains the z_1 component, i.e., depends on individual energies of two nucleons. This eigenvector is not considered in

Ref. [28].

In this section, the enlargement of the space of operators in the two-nucleon system in the $^1S_0$ channel is considered. We found a new kind of extended fixed objects which have (a) marginal direction(s). We then concentrated on the fixed point which is the most relevant to the realistic two-nucleon system, and found that the universal properties we got in the previous paper are unchanged under the enlargement of the space of operators, confirming that the approximation is reliable.

IV. HIGHER PARTIAL WAVES

Operators which contribute in higher partial waves contain more derivatives, and thus are less important at low energies. In a few instances, however, higher partial waves contain some interesting information. A well known example is the $p_{3/2}$ wave of the n-α system, where a narrow resonance state exists near the threshold, which is discussed in the NEFT context in Refs. [30, 31]. An important feature of this system is that there are *two* coupling constants to be fine-tuned. In the following, we will show that it comes out very naturally from our Wilsonian RG analysis. A similar analysis can be done for the D waves, and we show that, if there is a bound (or a resonance) state near the threshold, there are also *three* couplings to be fine-tuned.

A. P waves

In the NN system there are four channels in the P waves: $^1P_1$, $^3P_0$, $^3P_1$, and $^3P_2$-$^3F_2$, where we consider the mixing with an F wave for the $J = 2$ channel. For the $^1P_1$ channel, the interaction terms for the Γ_Λ may be written as

$$\Gamma_\Lambda^{int} = \int d^4x \left[- C_2^{(^1P_1)} \left(N^T P_i^{(^1P_1)} N \right)^\dagger \left(N^T P_i^{(^1P_1)} N \right) \right.$$
$$+ C_4^{(^1P_1)} \left\{ \left(N^T P_i^{(^1P_1)} N \right)^\dagger \left(N^T P_i^{(^1P_1)} \overleftrightarrow{\nabla}^2 N \right) + h.c. \right\}$$
$$\left. + 2 B_4^{(^1P_1)} \left[\left\{ N^T P_i^{(^1P_1)} \left(i\partial_t + \frac{\nabla^2}{2M} \right) N \right\}^\dagger \left(N^T P_i^{(^1P_1)} N \right) + h.c. \right] \right] \qquad (4.1)$$

up to including $\mathcal{O}(p^4)$, where $P_i^{(^1P_1)}$ is the projection operator to the $^1P_1$ channel, defined as

$$P_i^{(^1P_1)} = \frac{\sqrt{3}}{4\sqrt{2}} \overleftrightarrow{\nabla}_i (i\sigma_2)(i\tau_2). \tag{4.2}$$

Similarly, one can define the other projection operators,

$$P_a^{(^3P_0)} = \frac{1}{4\sqrt{2}} \overleftrightarrow{\nabla}_j (i\sigma_2\sigma_j)(i\tau_2\tau_a), \tag{4.3}$$

$$P_{ia}^{(^3P_1)} = \frac{\sqrt{3}}{8} \epsilon_{ikl} \overleftrightarrow{\nabla}_k (i\sigma_2\sigma_l)(i\tau_2\tau_a), \tag{4.4}$$

$$P_{ija}^{(^3P_2)} = \frac{\sqrt{3}}{8\sqrt{2}} \left[\overleftrightarrow{\nabla}_i (i\sigma_2\sigma_j) + \overleftrightarrow{\nabla}_j (i\sigma_2\sigma_i) - \frac{2}{3}\delta_{ij} \overleftrightarrow{\nabla}_k (i\sigma_2\sigma_k) \right] (i\tau_2\tau_a), \tag{4.5}$$

$$P_{ija}^{(^3F_2)} = \frac{5}{32} \left[\overleftrightarrow{\nabla}_i \overleftrightarrow{\nabla}_j \overleftrightarrow{\nabla}_l - \frac{1}{3}\left(\overleftrightarrow{\nabla}_i \delta_{jl} + \overleftrightarrow{\nabla}_j \delta_{li} + \overleftrightarrow{\nabla}_l \delta_{ij} \right) \overleftrightarrow{\nabla}^2 \right] (i\sigma_2\sigma_l)(i\tau_2\tau_a). \tag{4.6}$$

They are normalized in the same way as in Ref. [13],

$$\sum_{\text{pol.avg}} \text{Tr}\left[P^{(s)} P^{(s')\dagger} \right] = \frac{1}{2} |\boldsymbol{k}|^{2l} \delta_{ss'}, \tag{4.7}$$

where $\boldsymbol{k}$ is the relative three-momentum and l is the orbital angular momentum of the channel. For the P waves $l = 1$. The operators in another channel are obtained by replacing $P_i^{(^1P_1)}$ with the corresponding projection operator. In the $^3P_2$-$^3F_2$ channel, there is an additional operator,

$$C_4^{(^3F_2)} \left[\left(N^T P_{ija}^{(^3P_2)} N \right)^\dagger \left(N^T P_{ija}^{(^3F_2)} N \right) + h.c. \right], \tag{4.8}$$

which represents the mixing. Since the calculations are completely parallel, we will only demonstrate the results in the $P_i^{(^1P_1)}$ channel in the following.

We introduce the dimensionless coupling constants,

$$x_{(1,1)} = \frac{M\Lambda^3}{2\pi^2} C_2^{(^1P_1)}, \quad y_{(1,1)} = \frac{4M\Lambda^5}{2\pi^2} C_4^{(^1P_1)}, \quad z_{(1,1)} = \frac{\Lambda^5}{2\pi^2} B_4^{(^1P_1)}, \tag{4.9}$$

to write the following RG equations in the $n \to \infty$ limit,

$$\frac{dx_{(1,1)}}{dt} = -3x_{(1,1)} - \left[x_{(1,1)}^2 + 2x_{(1,1)}y_{(1,1)} + 2x_{(1,1)}z_{(1,1)} + y_{(1,1)}^2 + 2y_{(1,1)}z_{(1,1)} + z_{(1,1)}^2 \right], \tag{4.10}$$

$$\frac{dy_{(1,1)}}{dt} = -5y_{(1,1)} - \left[\frac{1}{2}x_{(1,1)}^2 + 2x_{(1,1)}y_{(1,1)} + \frac{3}{2}y_{(1,1)}^2 + y_{(1,1)}z_{(1,1)} - \frac{1}{2}z_{(1,1)}^2 \right], \tag{4.11}$$

$$\frac{dz_{(1,1)}}{dt} = -5z_{(1,1)} + \left[\frac{1}{2}x_{(1,1)}^2 + x_{(1,1)}y_{(1,1)} - x_{(1,1)}z_{(1,1)} + \frac{1}{2}y_{(1,1)}^2 - y_{(1,1)}z_{(1,1)} - \frac{3}{2}z_{(1,1)}^2 \right]. \tag{4.12}$$

17

We obtain the RGEs of the same form for the $^3P_0$ and $^3P_1$ channels with the coupling constants being suitably defined.

Compare them with the RGEs for the $^1S_0$ channel, (2.7), (2.8), and (2.9). With the appropriate replacement of the coupling constants, the coefficients of the quadratic terms are the same. Only the coefficients of the linear terms, which are nothing but the canonical dimensions of the corresponding operators, are different. This is because the channel dependence enters into the averaged action only through the projection operator and the canonical dimensions of the coupling constants. See the interaction part of Eq. (2.4) and Eq. (4.1), for example.

One can easily obtain the fixed points,

$$(x^\star, y^\star, z^\star) = (0, 0, 0), \quad \left(-3, \frac{9}{2}, -\frac{9}{2}\right), \quad \left(-\frac{25}{3}, \frac{35}{6}, -\frac{5}{2}\right). \tag{4.13}$$

We find that the scaling dimensions at the third fixed point are complex and may be disregarded.

It is useful to define the following variables,

$$u = x_{(1,1)}, \quad v = \frac{1}{2}\left(y_{(1,1)} - z_{(1,1)}\right), \quad w = \frac{1}{2}\left(y_{(1,1)} + z_{(1,1)}\right), \tag{4.14}$$

in terms of which the RG equations are written as

$$\frac{du}{dt} = -3u - (u + 2w)^2 \tag{4.15}$$

$$\frac{dv}{dt} = -5v - \frac{1}{2}(u + 4v)(u + 2w) \tag{4.16}$$

$$\frac{dw}{dt} = -5w - w(u + 2w) \tag{4.17}$$

The nontrivial fixed point is now at $(u^\star, v^\star, w^\star) = \left(-3, \frac{9}{2}, 0\right)$. Note that flows starting in the $w = 0$ plane never depart from it.

In Fig. 1, we show the RG flow in the $w = 0$ plane. It is easy to see that $u = -3$ is a phase boundary; the flows in the right of it (the weak coupling phase) run to the trivial fixed point, while those in the left of it (the strong coupling phase) go to infinity.

At the nontrivial fixed point, we can easily obtain the following scaling dimensions and corresponding eigenvectors (in the u, v, w basis),

$$\nu_1 = 3: \; \boldsymbol{u}_1 = \begin{pmatrix} 1 \\ -3 \\ 0 \end{pmatrix}, \quad \nu_2 = 1: \; \boldsymbol{u}_2 = \begin{pmatrix} 0 \\ 1 \\ 0 \end{pmatrix}, \quad \nu_3 = -2: \; \boldsymbol{u}_3 = \begin{pmatrix} 12 \\ -1 \\ -5 \end{pmatrix}. \tag{4.18}$$
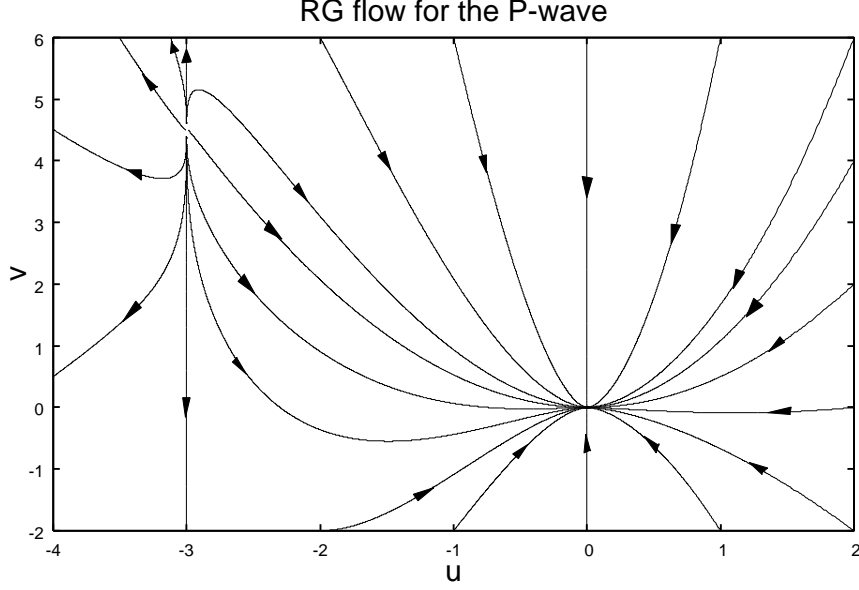
18

FIG. 1: The RG flow for the P wave in the $w = 0$ plane.

Note that there are two relevant directions, though they are all irrelevant at the trivial fixed point. For the first two eigenvectors, the scaling dimensions shift from their canonical values by six.

We can investigate the $^3P_2$-$^3F_2$ channel in a similar way. After introducing dimensionless couplings,

$$x_{(3,2)} = \frac{M\Lambda^3}{2\pi^2} C_2^{(^3P_2)}, \quad y_{(3,2)} = \frac{4M\Lambda^5}{2\pi^2} C_4^{(^3P_2)},$$
$$z_{(3,2)} = \frac{\Lambda^5}{2\pi^2} B_4^{(^3P_2)}, \quad w_{(3,2)} = \frac{\sqrt{2}}{2} \frac{M\Lambda^5}{2\pi^2} C_4^{(^3F_2)}, \tag{4.19}$$

we have (in the $n \to \infty$ limit)

$$\frac{dx_{(3,2)}}{dt} = -3x_{(3,2)} - \left[x_{(3,2)}^2 + 2x_{(3,2)}y_{(3,2)} + 2x_{(3,2)}z_{(3,2)} + y_{(3,2)}^2 + 2y_{(3,2)}z_{(3,2)} + z_{(3,2)}^2 + 2w_{(3,2)}^2 \right],$$
$$\tag{4.20}$$

$$\frac{dy_{(3,2)}}{dt} = -5y_{(3,2)} - \left[\frac{1}{2}x_{(3,2)}^2 + 2x_{(3,2)}y_{(3,2)} + \frac{3}{2}y_{(3,2)}^2 + y_{(3,2)}z_{(3,2)} - \frac{1}{2}z_{(3,2)}^2 + w_{(3,2)}^2 \right], \tag{4.21}$$

$$\frac{dz_{(3,2)}}{dt} = -5z_{(3,2)} + \left[\frac{1}{2}x_{(3,2)}^2 + x_{(3,2)}y_{(3,2)} - x_{(3,2)}z_{(3,2)} + \frac{1}{2}y_{(3,2)}^2 - y_{(3,2)}z_{(3,2)} - \frac{3}{2}z_{(3,2)}^2 + w_{(3,2)}^2 \right],$$
$$\tag{4.22}$$

$$\frac{dw_{(3,2)}}{dt} = -5w_{(3,2)} - \left[x_{(3,2)}w_{(3,2)} + y_{(3,2)}w_{(3,2)} + z_{(3,2)}w_{(3,2)} \right]. \tag{4.23}$$

Note that, with the appropriate replacement of the coupling constants, the coefficients of the quadratic terms of the above RGEs are the same as those in the ${}^3S_1$-${}^3D_1$ channel, and the only difference is the coefficients of the linear terms representing the canonical dimensions, just as we explained for the ${}^1P_1$ and ${}^1S_0$ channels. The flows and the scaling dimensions are similar to those for other P waves, just as those for the ${}^3S_1$-${}^3D_1$ channel to those of ${}^1S_0$.

B.   Amplitude for the P waves

Similar results may be obtained by explicitly calculating the scattering amplitude as we did for the S-waves in Refs. [18, 34], which is the extention of the method in Refs. [11, 41] to include the redundant operators. Consider the Lippmann-Schwinger equation with the "potential" in the center-of-mass frame (See Appendix A),

$$- iV = -iP^\dagger \otimes P \left(-4\boldsymbol{p}_1 \cdot \boldsymbol{p}_2\right) \left[C_2 + 4C_4 \left(\boldsymbol{p}_1^2 + \boldsymbol{p}_2^2\right) - 2B_4 \left(p^0 - \frac{\boldsymbol{p}_1^2 + \boldsymbol{p}_2^2}{2M}\right)\right], \qquad (4.24)$$

where $\boldsymbol{p}_1$ and $\boldsymbol{p}_2$ are momenta of the nucleons in the initial and final states respectively, P stands for the spin-isospin factor of the projection operator (for example, $P = \frac{\sqrt{3}}{4\sqrt{2}}\sigma_2\tau_2$ for the ${}^1P_1$ channel), and the ansatz for the amplitude,

$$- i\mathcal{A} = -iP^\dagger \otimes P \left(-4\boldsymbol{p}_1 \cdot \boldsymbol{p}_2\right) \left[X(p^0) + Y(p^0) \left(\boldsymbol{p}_1^2 + \boldsymbol{p}_2^2\right) + Z(p^0)\boldsymbol{p}_1^2\boldsymbol{p}_2^2\right], \qquad (4.25)$$

where $X(p^0)$, $Y(p^0)$, and $Z(p^0)$ are functions to be determined. The Lippmann-Schwinger equation reduces to

$$- i\tilde{\mathcal{A}}(p^0, p_1, p_2) = -i\tilde{V}(p^0, p_1, p_2) + \int \frac{d^3k}{(2\pi)^3} \left(-i\tilde{V}(p^0, k, p_2)\right) \frac{ik^2}{p^0 - \frac{k^2}{M} + i\epsilon} \left(-i\tilde{\mathcal{A}}(p^0, p_1, k)\right), \qquad (4.26)$$

where we have introduced

$$\tilde{\mathcal{A}} = \left[X(p^0) + Y(p^0) \left(\boldsymbol{p}_1^2 + \boldsymbol{p}_2^2\right) + Z(p^0)\boldsymbol{p}_1^2\boldsymbol{p}_2^2\right], \qquad (4.27)$$

$$\tilde{V} = \left[C_2 + 4C_4 \left(\boldsymbol{p}_1^2 + \boldsymbol{p}_2^2\right) - 2B_4 \left(p^0 - \frac{\boldsymbol{p}_1^2 + \boldsymbol{p}_2^2}{2M}\right)\right]. \qquad (4.28)$$

The solution is easily obtained as,

$$X = \frac{1}{D} \left[(C_2 - 2B_4 p^0) + \left(4C_4 + \frac{B_4}{M}\right)^2 I_3\right], \qquad (4.29)$$

$$Y = \frac{1}{D} \left(4C_4 + \frac{B_4}{M}\right) \left[1 - \left(4C_4 + \frac{B_4}{M}\right) I_2\right], \qquad (4.30)$$

$$Z = \frac{1}{D} \left(4C_4 + \frac{B_4}{M}\right)^2 I_1, \qquad (4.31)$$

20

with

$$D = 1 - \left(C_2 - 2B_4 p^0\right) I_1 - 2\left(4C_4 + \frac{B_4}{M}\right) I_2$$
$$+ \left(4C_4 + \frac{B_4}{M}\right)^2 I_2^2 - \left(4C_4 + \frac{B_4}{M}\right)^2 I_1 I_3, \tag{4.32}$$

where

$$I_n = -\frac{M}{2\pi^2} \int_0^\Lambda dk \frac{k^{2n+2}}{k^2 + \mu^2}, \quad \mu = \sqrt{-Mp^0 - i\epsilon}. \tag{4.33}$$

The RG equation may be obtained by requiring the amplitude to be independent of the cutoff Λ. By introducing

$$\mathcal{X} = 1 + \frac{2}{5}w, \quad \mathcal{Y} = u - \frac{4}{7}w^2, \quad \mathcal{Z} = 2(v + w) + \frac{4}{5}w^2, \tag{4.34}$$

we find the following RG equations,

$$\Lambda \frac{d\mathcal{X}}{d\Lambda} = \frac{1}{\mathcal{X}}\left(\mathcal{X} - 1\right)\left(5\mathcal{X}^2 + \mathcal{Y}\right), \tag{4.35}$$

$$\Lambda \frac{d\mathcal{Y}}{d\Lambda} = \frac{\mathcal{Y}}{\mathcal{X}^2}\left(10\mathcal{X}^3 - 7\mathcal{X}^2 + 2\mathcal{X}\mathcal{Y} - \mathcal{Y}\right), \tag{4.36}$$

$$\Lambda \frac{d\mathcal{Z}}{d\Lambda} = \frac{1}{\mathcal{X}^2}\left(\mathcal{Y}^2 - 5\mathcal{X}^2\mathcal{Z} + 10\mathcal{X}^3\mathcal{Z} + 2\mathcal{X}\mathcal{Y}\mathcal{Z}\right), \tag{4.37}$$

which give rise to the following fixed points,

$$(\mathcal{X}^\star, \mathcal{Y}^\star, \mathcal{Z}^\star) = (1, 0, 0), \quad (1, -3, 9). \tag{4.38}$$

In the original variables, they are

$$(u^\star, v^\star, w^\star) = (0, 0, 0), \quad \left(-3, \frac{9}{2}, 0\right), \tag{4.39}$$

consistent with the previous analysis using the Legendre flow equation. Note that there are no additional nontrivial fixed points.

At the nontrivial fixed point, we can obtain the scaling dimensions and the corresponding eigenvectors (in the u, v, w basis),

$$\nu_1 = 3: \ \boldsymbol{u}_1 = \begin{pmatrix} 1 \\ -3 \\ 0 \end{pmatrix}, \quad \nu_2 = 1: \ \boldsymbol{u}_2 = \begin{pmatrix} 0 \\ 1 \\ 0 \end{pmatrix}, \quad \nu_3 = -2: \ \boldsymbol{u}_3 = \begin{pmatrix} 12 \\ -13 \\ -5 \end{pmatrix}. \tag{4.40}$$

Compare the results with (4.18). The scaling dimensions agree and the only difference is the eigenvector for ν_3. We have seen a similar phenomenon for the $^1S_0$ channel, as we explained in Sec. II C.

By substituting

$$\begin{pmatrix} \delta u \\ \delta v \\ \delta w \end{pmatrix} = a\boldsymbol{u}_1 \left(\frac{\Lambda_0}{\Lambda}\right)^3 + b\boldsymbol{u}_2 \left(\frac{\Lambda_0}{\Lambda}\right) + c\boldsymbol{u}_3 \left(\frac{\Lambda}{\Lambda_0}\right)^2 \tag{4.41}$$

into the amplitude, we obtain the off-shell amplitude near the nontrivial fixed point,

$$\tilde{\mathcal{A}}^{-1}(p^0, \boldsymbol{p}_1, \boldsymbol{p}_2)\Big|_* = -\frac{M\Lambda_0^3}{2\pi^2}\left(\frac{a}{9}\right) + \frac{M\Lambda_0}{2\pi^2}\left(-\frac{2b}{9}\right)\mu^2 + \cdots + \frac{M}{4\pi}\mu^3, \tag{4.42}$$

where the ellipsis stands for higher order terms in a, b, and c. By comparing it with the effective range expansion,

$$\tilde{\mathcal{A}}^{-1} = -\frac{M}{4\pi}\left[-\frac{1}{\alpha} + \frac{r}{2}p^2 + \cdots - ip^3\right], \tag{4.43}$$

defined on the mass shell, one sees

$$\alpha^{-1} = -\frac{2\Lambda_0^3}{9\pi}a, \quad r = -\frac{8\Lambda_0}{9\pi}b. \tag{4.44}$$

Namely, the two relevant directions correspond to the "scattering length" α and the "effective range" r. (These effective range parameters have different dimensionality in the P waves from those in the S waves.) Note that the strong coupling phase ($a < 0$) corresponds to a positive "scattering length," and the weak coupling phase ($a > 0$) corresponds to a negative one.

In Ref. [30] it is noticed that there are two couplings to be fine-tuned. They corresponds to our relevant parameters given above. We have given the explanation for what they found from the RG point of view.

In order to understand the difference between the strong and the weak coupling phases, we take a closer look at the poles of the amplitude in the effective range expansion. Note that we are in the vicinity of the nontrivial fixed point, i.e., $|a| \ll 1$ and $|b| \ll 1$. At low energies, the poles are the solutions of the cubic equation [30],

$$-\frac{1}{\alpha} + \frac{r}{2}p^2 - ip^3 = 0. \tag{4.45}$$

Note that if we change the signs of α and r simultaneously, $\alpha \to -\alpha$ and $r \to -r$, the solutions are given by $p \to p^*$.
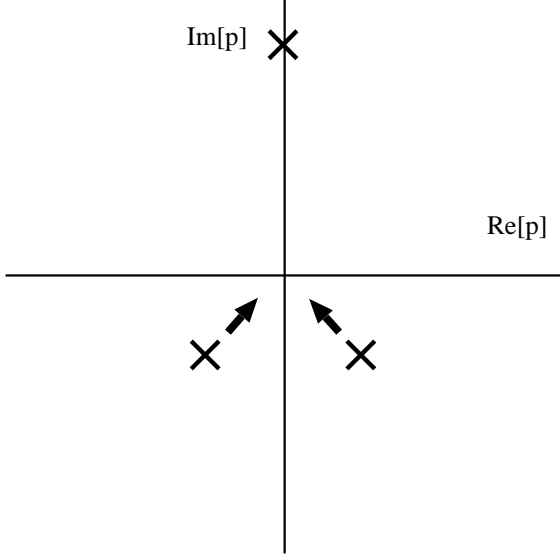
FIG. 2: Poles for small $\alpha^{-1} < 0$ and $r < 0$. The arrows indicate the directions to which the poles move as $\alpha^{-1} \to 0-$. There is a shallow resonance.
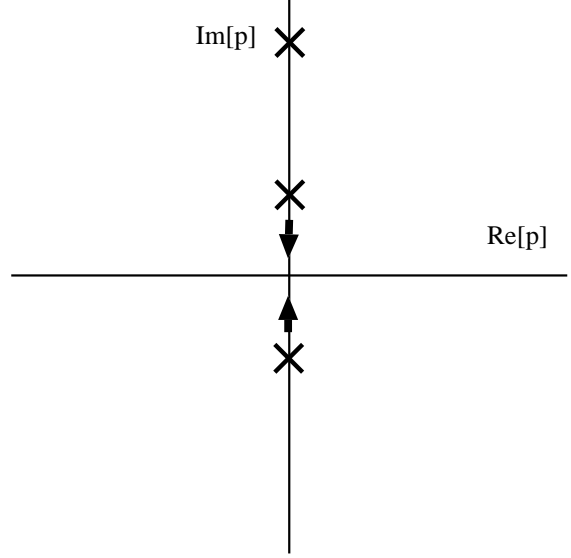

FIG. 3: Poles for small $\alpha^{-1} > 0$ and $r < 0$. The arrows indicate the directions to which the poles move as $\alpha^{-1} \to 0+$. There is a shallow bound state.

Let us first suppose that we are in the region $\alpha^{-1} < 0$ but not very close to the critical value $|\alpha^{-1}| = 0$, i.e., $|\alpha r^3| < 54$. In this case, we have three solutions,

$$\pm \frac{\sqrt{3}}{12}\left(\frac{|\alpha|^{\frac{1}{3}} r^2}{v} - \frac{v}{|\alpha|^{\frac{1}{3}}}\right) - \frac{i}{6}\left(r + \frac{|\alpha|^{\frac{1}{3}} r^2}{2v} + \frac{v}{2|\alpha|^{\frac{1}{3}}}\right), \quad -\frac{i}{6}\left(r - \frac{|\alpha|^{\frac{1}{3}} r^2}{v} - \frac{v}{|\alpha|^{\frac{1}{3}}}\right). \quad (4.46)$$

where

$$v \equiv \left[108 + \alpha r^3 + 108\sqrt{1 + \frac{\alpha r^3}{54}}\right]^{\frac{1}{3}} \quad (4.47)$$

is a positive number. These poles are in most cases unimportant in low-energy scattering. Only when we take the limit $\alpha^{-1} \to 0$ and $r \to 0$ keeping the condition $|\alpha r^3| < 54$, all of the three poles move closer to the origin and they become significant. The very existence of such a special limit is a consequence of the two relevant directions. Note that this limit is a simultaneous limit $a \to 0$ and $b \to 0$ with keeping $|b^3/a|$ "small", i.e., $|b^3/a| < 2187\pi^2/128 \approx 168.5$. We do not consider such a case here, but approach to the critical value $\alpha^{-1} \to 0-$ keeping r finite. This is the limit $a \to 0$ keeping b finite so that $|b^3/a| \to \infty$. The discussion about these limits and the relations to the power counting suggested in Refs. [30, 31] is given in Sec. V.

23

If $r < 0$, the expression for the solutions of Eq. (4.46) is still valid for $|\alpha r^3| > 54$. The first two poles in Eq. (4.46) move toward the origin as we decrease the magnitude of α^{-1} and reach it at $\alpha^{-1} = 0$ (See Fig. 2), while the third one does not move so much. This fairly deeply bound state is insignificant for low-energy scattering. Note that the first two poles represent a shallow resonance.

If we go across the critical value $\alpha^{-1} = 0$ into the region where $\alpha^{-1} > 0$, the two (degenerate) poles at the origin split on the imaginary axis. We have the solutions

$$-\frac{i}{6}r\left(1 + 2\sin\left(\frac{\phi}{3}\right)\right), \quad -\frac{i}{6}r\left(1 \pm \sqrt{3}\cos\left(\frac{\phi}{3}\right) - \sin\left(\frac{\phi}{3}\right)\right), \qquad (4.48)$$

where

$$\phi = \mathrm{Arg}\left[\left(108 + \alpha r^3\right)i + 108\sqrt{-\left(1 + \frac{\alpha r^3}{54}\right)}\right]. \qquad (4.49)$$

The first pole represents a shallow bound state. See Fig. 3. The pole with the positive sign of the second corresponds to the bound state found in the $\alpha^{-1} < 0$ case. The pole with the negative sign of the second does not seem to have a definite physical meaning, but is responsible for the rapid change of the phase shift at low momenta.

Note that there are several cases (the case with $r > 0$ and $\alpha > 0$ and the case with $r < 0$, $\alpha > 0$, and $|\alpha r^3| < 54$) in which the poles appear on the upper half plane, but causality prohibits poles on the upper half plane except on the imaginary axis [42, 43, 44, 45]. One should therefore exclude such regions of a and b which give rise to acausal poles. See Refs. [46, 47, 48, 49, 50, 51] for the cases where some physical axioms such as causality, positivity and unitarity constrain the values of low-energy constants. Remember that we have assumed that $|a| \ll 1$ and $|b| \ll 1$ (and $|b^3/a|$ is large), that is, $|\alpha^{-1}| \ll \Lambda_0^3$ and $|r| \ll \Lambda_0$, with $|\alpha r^3|$ being large, through the analysis to meet the condition that we are in the vicinity of the nontrivial fixed point. The poles we have discussed have magnitudes smaller than the cutoff Λ_0 to be consistent with the effective range expansion.

To summarize, we have done the RG analysis based on the cutoff independence of the amplitude, and found that, near the nontrivial fixed point, the scattering length and the effective range are related to the deviations a and b from the nontrivial fixed point. The amplitude has three poles at low momenta. Two of the three poles are sensitive to the value of α^{-1} and get close to the origin near the critical value. For $r < 0$, there is a shallow resonance in the weak coupling phase $a > 0$ ($\alpha^{-1} < 0$), and a shallow bound state in the strong coupling phase $a < 0$ ($\alpha^{-1} > 0$). The appearance of a (shallow) bound state in the

24

strong coupling phase is similar to that in the S waves. But the appearance of a (shallow) resonance is a new feature which is absent in the S waves.

C. D waves

There are four channels in the D waves; $^1D_2$, $^3D_1$, $^3D_2$, and $^3D_3$-$^3G_3$, the second of which mixes with $^3S_1$ and has been considered. We introduce the following projection operators,

$$
\begin{aligned}
P_{ija}^{(^1D_2)} =& \frac{\sqrt{15}}{16} \left(\overleftrightarrow{\nabla}_i \overleftrightarrow{\nabla}_j - \frac{1}{3} \overleftrightarrow{\nabla}^2 \delta_{ij} \right) (i\sigma_2)(i\tau_2\tau_a), \\
P_{ij}^{(^3D_2)} =& \frac{\sqrt{5}}{16\sqrt{2}} \left[\epsilon_{imn} \overleftrightarrow{\nabla}_m \overleftrightarrow{\nabla}_j + \epsilon_{jmn} \overleftrightarrow{\nabla}_m \overleftrightarrow{\nabla}_i \right] (i\sigma_2\sigma_n)(i\tau_2), \\
P_{ijk}^{(^3D_3)} =& \frac{\sqrt{15}}{48} \left[\left\{ \left(\overleftrightarrow{\nabla}_i \overleftrightarrow{\nabla}_j - \frac{1}{3} \overleftrightarrow{\nabla}^2 \delta_{ij} \right) (i\sigma_2\sigma_k) + (\text{cyclic in } i,j,k) \right\} \right. \\
& \left. - \frac{2}{5} \left\{ \left(\overleftrightarrow{\nabla}_k \overleftrightarrow{\nabla}_l - \frac{1}{3} \overleftrightarrow{\nabla}^2 \delta_{kl} \right) \delta_{ij} + (\text{cyclic in } i,j,k) \right\} (i\sigma_2\sigma_l) \right] (i\tau_2), \\
P_{ijk}^{(^3G_3)} =& \frac{7\sqrt{5}}{128} \left[\overleftrightarrow{\nabla}_i \overleftrightarrow{\nabla}_j \overleftrightarrow{\nabla}_k \overleftrightarrow{\nabla}_l - \frac{1}{7} \overleftrightarrow{\nabla}^2 \left(\overleftrightarrow{\nabla}_i \overleftrightarrow{\nabla}_j \delta_{kl} + (\text{5 terms to be symmetric in } i,j,k,l) \right) \right. \\
& \left. + \frac{1}{35} \overleftrightarrow{\nabla}^4 \left(\delta_{ij}\delta_{kl} + \delta_{ik}\delta_{jl} + \delta_{il}\delta_{jk} \right) \right] (i\sigma_2\sigma_l)(i\tau_2).
\end{aligned}
\tag{4.50}
$$

Because the RG equations are the same for both $^1D_2$ and $^3D_2$ channels, we present the calculation for the $^1D_2$ channel only. (Those for the coupled channel $^3D_3$-$^3G_3$ are similar to those for the $^3S_1$-$^3D_1$ and the $^3P_2$-$^3F_2$ channels that we do not show them explicitly.) For this channel, the interaction terms for the Γ_Λ up to $\mathcal{O}(p^6)$ may be written as

$$
\begin{aligned}
\Gamma_\Lambda^{int} = \int d^4x \left[\right. & -C_4^{(^1D_2)} \left(N^T P_{ija}^{(^1D_2)} N \right)^\dagger \left(N^T P_{ija}^{(^1D_2)} N \right) \\
& + C_6^{(^1D_2)} \left\{ \left(N^T P_{ija}^{(^1D_2)} N \right)^\dagger \left(N^T P_{ija}^{(^1D_2)} \overleftrightarrow{\nabla}^2 N \right) + h.c. \right\} \\
& \left. + 2B_6^{(^1D_2)} \left[\left(N^T P_{ija}^{(^1D_2)} N \right)^\dagger \left\{ N^T P_{ija}^{(^1D_2)} \left(i\partial_t + \frac{\nabla^2}{2M} \right) N \right\} + h.c. \right] \right].
\end{aligned}
\tag{4.51}
$$

In terms of the dimensionless coupling constants,

$$
x_{(1,2)} = \frac{M\Lambda^5}{2\pi^2} C_4^{(^1D_2)}, \quad y_{(1,2)} = \frac{4M\Lambda^7}{2\pi^2} C_6^{(^1D_2)}, \quad z_{(1,2)} = \frac{\Lambda^7}{2\pi^2} B_6^{(^1D_2)},
\tag{4.52}
$$

25

we find the following RG equations (in the $n \to \infty$ limit),

$$\frac{dx_{(1,2)}}{dt} = -5x_{(1,2)} - \left[x_{(1,2)}^2 + 2x_{(1,2)}y_{(1,2)} + 2x_{(1,2)}z_{(1,2)} + y_{(1,2)}^2 + 2y_{(1,2)}z_{(1,2)} + z_{(1,2)}^2\right],$$

$$\frac{dy_{(1,2)}}{dt} = -7y_{(1,2)} - \left[\frac{1}{2}x_{(1,2)}^2 + 2x_{(1,2)}y_{(1,2)} + \frac{3}{2}y_{(1,2)}^2 + y_{(1,2)}z_{(1,2)} - \frac{1}{2}z_{(1,2)}^2\right],$$

$$\frac{dz_{(1,2)}}{dt} = -7z_{(1,2)} + \left[\frac{1}{2}x_{(1,2)}^2 + x_{(1,2)}y_{(1,2)} - x_{(1,2)}z_{(1,2)} + \frac{1}{2}y_{(1,2)}^2 - y_{(1,2)}z_{(1,2)} - \frac{3}{2}z_{(1,2)}^2\right].$$

$$(4.53)$$

Just as for the $^1P_1$ case, with the appropriate replacement of the coupling constants, the coefficients of the quadratic terms of the above RGEs are the same as those in the $^1S_0$ channel, and the only difference is the coefficients of the linear terms representing the canonical dimensions.

The nontrivial fixed points are found to be

$$\left(x_{(1,2)}^\star, y_{(1,2)}^\star, z_{(1,2)}^\star\right) = (0,0,0), \quad \left(-5, \frac{25}{6}, -\frac{25}{6}\right), \quad \left(-\frac{49}{5}, \frac{63}{10}, -\frac{7}{2}\right), \qquad (4.54)$$

but the last nontrivial fixed point has complex scaling dimensions, and thus may be disregarded. At the nontrivial fixed point, $\left(-5, \frac{25}{6}, -\frac{25}{6}\right)$, we find the following scaling dimensions and the corresponding eigenvectors,

$$\nu_1 = 5: \ u_1 = \begin{pmatrix} 3 \\ -5 \\ 5 \end{pmatrix}, \quad \nu_2 = 3: \ u_2 = \begin{pmatrix} 0 \\ -1 \\ 1 \end{pmatrix}, \quad \nu_3 = -2: \ u_3 = \begin{pmatrix} -10 \\ 5 \\ 2 \end{pmatrix}. \qquad (4.55)$$

Note that there are two relevant couplings. For the first two eigenvectors, the scaling dimensions shift from their canonical values by ten.

To summarize, we have examined the D waves in the similar way, and found that there are two relevant couplings with the scaling dimensions shifted by ten. These large anomalous dimensions suggest that there may be more relevant operators. In the next section, we give another guide for what we expect for scaling dimensions from a different point of view, and show that there is one more relevant operator.

D. PDS for higher partial waves

In the previous paper [18], we explain how the PDS leads to the "shift by two" rule for the S waves, that is, the anomalous dimensions of the four nucleon operators are two. In

short, the usual PDS renormalization, which subtracts the contribution at the $D = 3$ pole as well, treats the operators *as if they were in three dimensional spacetime.* The canonical dimensions of the four-nucleon operators shift by two, e.g., the operator $(N^T N)^\dagger (N^T N)$ has dimension six in $(1 + 3)$ dimensions, but four in $(1 + 2)$ dimensions. (In D dimensions, it has dimension $2(D - 1)$.)

Note that this "shift rule" does not apply to the redundant operators, which do not need to be introduced with the dimensional regularization.

We have seen that the rule for the P waves is "shift by six," and for the D waves, "shift by ten." It is now natural to extend the PDS scheme to higher partial waves by subtracting the contribution at $D = 1$ for the P waves, and that at $D = -1$ for the D waves.

One can easily show that this generalization of PDS for higher partial waves works well as for the S waves in the pionless NEFT.

This kind of generalization of PDS has been considered in Ref. [52] but apparently the relevance to higher partial waves was not noticed.

Guided by this extended PDS prescription, we expect that there should be one more relevant operator (with the scaling dimension one) in the D waves, even though we found only two relevant operators in the previous subsection. The operator will be found if one performs a similar analysis in larger operator space.

Note that the RGEs for the P and D waves have the similar structure to those for the S waves, as we remarked in Sec. IV A and in Sec. IV C. The RGEs for the D waves to $\mathcal{O}(p^8)$ should be obtained from those for the S waves to $\mathcal{O}(p^4)$ given in Sec. III B by replacing the coefficients of the linear terms with the corresponding ones for the D waves (which are nothing but the canonical dimensions), with appropriate replacement of the coupling constants. By examining the RGEs, one can immediately obtain the nontrivial fixed point,

$$\left(-5, \frac{25}{6}, -\frac{25}{6}, 0, \frac{100}{9}, 0, -\frac{100}{9}, -\frac{100}{9}\right), \tag{4.56}$$

where the first three components are $(x_{(1,2)}, y_{(1,2)}, z_{(1,2)})$, while the rest are the dimensionless coupling constants of $\mathcal{O}(p^8)$.

By solving the linearized RGEs around it, we obtain the following eigenvalues and eigen-

vectors,

$$\nu_1 = +5: \quad \boldsymbol{u}_1 = \left(\frac{3}{5}, -1, 1, 0, -1, 0, 1, 1\right), \tag{4.57}$$

$$\nu_2 = +3: \quad \boldsymbol{u}_2 = \left(0, \frac{3}{20}, -\frac{3}{20}, 0, -1, 0, 1, 1\right), \tag{4.58}$$

$$\nu_3 = +1: \quad \boldsymbol{u}_3 = (0, 0, 0, 0, -1, 0, 1, 1), \tag{4.59}$$

$$\nu_4 = -2: \quad \boldsymbol{u}_4 = \left(-\frac{54}{127}, \frac{90}{127}, -\frac{261}{635}, 0, -\frac{190}{127}, 0, \frac{64}{127}, 1\right), \tag{4.60}$$

$$\nu_5 = -4: \quad \boldsymbol{u}_5 = \left(-\frac{30}{37}, \frac{25}{37}, -\frac{25}{37}, \frac{27}{37}, -2, 0, 0, 1\right), \tag{4.61}$$

$$\nu_6 = -4: \quad \boldsymbol{u}_6 = \left(-\frac{45}{74}, -\frac{55}{74}, \frac{55}{74}, \frac{81}{148}, 1, 0, 1, 0\right), \tag{4.62}$$

$$\nu_7 = -4: \quad \boldsymbol{u}_7 = \left(-\frac{45}{37}, -\frac{55}{37}, \frac{55}{37}, \frac{155}{74}, 0, 1, 0, 0\right), \tag{4.63}$$

$$\nu_8 = -9: \quad \boldsymbol{u}_8 = \left(\frac{9}{8}, -\frac{15}{8}, \frac{3}{10}, 0, \frac{13}{8}, 0, \frac{71}{50}, 1\right). \tag{4.64}$$

We find the third relevant operator as we expected. The extended PDS prescription and the Wilsonian RG analysis given above give a consistent result.

V. SUMMARY AND DISCUSSION

In this paper, we extend our previous study of the Wilsonian RG analysis for the pionless NEFT in the two-nucleon sector. The determination of power counting based on the scaling dimensions is a simple and powerful method in particular for the theories in which nonperturbative dynamics is important.

Two kinds of extensions are considered; (1) enlargement of the space of operators to be taken into account, and (2) higher partial waves. Because our formulation is general, we can use the same machinery to analyze them.

We considered the space of operators up to including those of $\mathcal{O}(p^4)$ in the $^1S_0$ channel and found that the results are stable against the enlargement. We also found that there are "fixed lines" and a "fixed surface" which are related to the existence of marginal operators.

In the P and D waves, we derived the RG equations and found the phase structures. There are two phases, the strong coupling and the weak coupling phases, just as in the S waves. Unlike the case of the S waves, however, there are two relevant directions at the nontrivial fixed point for the P waves. We found that there are three for the D waves.

By explicitly calculating the off-shell amplitude for the P waves, we have seen that (near the critical surface and $r < 0$) there is a shallow bound state in the strong coupling phase, while in the weak coupling phase there is a shallow resonance.

To summarize, we have a coherent picture of the pionless NEFT in the two-nucleon sector from the Wilsonian RG point of view.

In the following, we discuss several aspects of the results.

1. In the enlarged space calculation, we found "fixed lines" and a "fixed surface." At first sight, they seem very strange. But actually, their existence is related to that of marginal operators. In relativistic field theory, classically marginal operators usually get (non-integer) anomalous dimensions and turn into relevant or irrelevant operators, so that the corresponding coupling constants run though slowly. In the present case, we have no logarithmic divergences so that the marginal operators are really marginal. Their couplings do not run at all.

2. The absence of logarithmic divergences seems to lead to integer scaling dimensions. We found however that "fixed surface" [F] has irrational scaling dimensions. This fact tempts us to think that it is an artefact.

3. The additional nontrivial fixed point found in Ref. [18], which has complex scaling dimensions, disappears in the enlarged space calculation. It is well known that the truncation in general produces spurious solutions [35, 37]. It is also known that truncation leads to complex scaling dimensions. (Note that the RG equations obtained from amplitudes do not have such spurious fixed points.) As we discussed in Sec. III B, those fixed points with complex scaling dimensions are considered as spurious. Note however that what we are doing is not the so-called *polynomial expansion* (the expansion in powers of fields), but the *derivative expansion* only. It is due to the Fermi-Dirac statistics and the nonrelativistic feature that there are only a finite number of interaction terms in the derivative expansion to a given order. It is remarkable that the derivative expansion shows the similar symptom to that of the polynomial expansion seen in relativistic scalar theory.

4. As we discussed in a previous paper [18], some of the eigenvectors seem to correspond to the directions in which the physical quantities remain unchanged. We suspect that

the eigenvectors with scaling dimensions which do not obey the "shift by two" rule in the S waves are such directions, and that there is a similar correspondence in each partial wave.

5. In the P wave calculation, we found that there are two relevant operators in a very natural way. The fact that there are two couplings to be fine-tuned has been noticed in Ref. [30]. It requires a nonperturbative analysis to decide which couplings should be treated nonperturbatively and cannot be determined by perturbative considera- tion. In fact, they showed that two couplings should be fine-tuned by the explicit (nonperturbative) calculation using a dimeron.

6. In Ref. [30], the case

$$\alpha^{-1} \sim M_{lo}^3, \quad r \sim M_{lo}, \quad \text{so that} \quad \left| \alpha r^3 \right| \sim \mathcal{O}(1) \tag{5.1}$$

is considered as an unnatural case, where M_{lo} is a low-energy scale. In Ref. [31], on the other hand, another power counting is considered, in which only one combination of coupling constants is fine-tuned,

$$\alpha^{-1} \sim M_{lo}^2 M_{hi}, \quad r \sim M_{hi}, \quad \text{so that} \quad \left| \alpha r^3 \right| \sim \mathcal{O}\left(\frac{M_{hi}^2}{M_{lo}^2} \right) \gg 1 \tag{5.2}$$

where M_{hi} is a high-energy scale. The former case corresponds to the special limit mentioned in Sec. IV B, in which α^{-1} is sent to zero, keeping $\left| \alpha r^3 \right| < 54$. All of the three poles move closer to the origin, thus they become significant in low-energy scattering. The latter corresponds to the limit in which $\alpha^{-1} \to 0$ keeping r finite, so that $\left| \alpha r^3 \right| > 54$. Only two poles (representing a resonance in the weak coupling phase) move closer to the origin, while the third is insignificant. In terms of the phase diagram, this corresponds to the flows very close to the phase boundary, but not to the fixed point itself.

7. In the real world, the two-nucleon system in the P waves does not exhibit any shallow resonances nor bound states, so that it is in the weak coupling phase. There may be systems which can be described by the same EFT at low energies. For example, Feshbach resonances of ultracold ^{40}K [53] or ^{6}Li [54, 55] may be interesting.

APPENDIX A: RELATION BETWEEN THE LEGENDRE FLOW EQUATION IN THE SHARP CUTOFF LIMIT AND THE RG EQUATION BY BIRSE ET AL.

1. Feynman rules

Legendre flow equation reduces to a set of RG equations for coupling constants, which consists of one-loop diagrams. In the present case, a typical diagram is given in Fig. 4. Let us first describe the Feynman rules for the $^1S_0$ channel as an example. From the averaged action, one can easily read off the Feynman rules for the vertex (See Fig. 5),

$$4ix_A F_A(p_f, p_i) \left(P_a^\dagger\right)_{kl} (P_a)_{ij} , \tag{A1}$$

where x_A is a dimensionless coupling constant. For the $^1S_0$ channel, it is one of the dimensionless coupling constants introduced in (3.7), $x_A \in \{x, y, z, u_1, u_2, z_1, z_2, z_3\}$. $(P_a)_{ij}$ is the spin-isospin factor of the projection operator to the partial wave in question, with the indices i and j referring to the spin and isospin quantum numbers of the nucleon pair. $F_A(p_f, p_i)$ is the corresponding momentum-dependent factor to x_A, where p_i stands for the incoming momenta, while p_f for the outgoing ones. For the $^1S_0$ channel, we have

$$F_x = \frac{-2\pi^2}{M\Lambda}, \quad F_y = \frac{-2\pi^2}{4M\Lambda^3} (r_{12} + r_{34}), \quad F_z = \frac{2\pi^2}{\Lambda^3} \sum_{i=1}^4 S_i,$$

$$F_{u_1} = \frac{-2\pi^2}{16M\Lambda^5} \left(r_{12}^2 + r_{34}^2\right), \quad F_{u_2} = \frac{-2\pi^2}{16M\Lambda^5} r_{12} r_{34},$$

$$F_{z_1} = \frac{2\pi^2 M}{\Lambda^5} \sum_{i=1}^4 S_i^2, \quad F_{z_2} = \frac{2\pi^2 M}{\Lambda^5} (S_1 + S_2)(S_3 + S_4),$$

$$F_{z_3} = \frac{2\pi^2}{4\Lambda^5} \left\{r_{12}(S_3 + S_4) + r_{34}(S_1 + S_2)\right\}. \tag{A2}$$

Note that r_{ij} and S_i are defined in Eq. (3.6).

2. Subtleties at equal times

When we include higher order redundant operators, we encounter subtleties which do not emerge in the lowest order. In this subsection, we explain the subtleties and how to handle them.
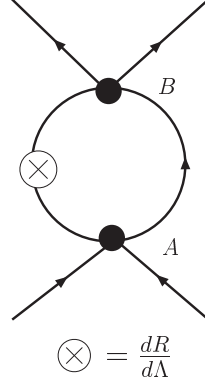
FIG. 4: One-loop diagram contributing to the Legendre flow equation. Labels A and B stand for the type of the vertices. The A vertex is given in FIG. 5.
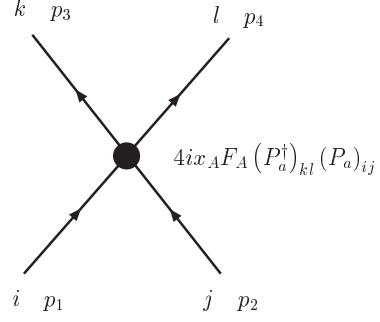

FIG. 5: Feynman rule for a vertex labeled by A, where i, j, etc. are the spin-isospin indices, and p_k ($k = 1, 2, 3, 4$) are momenta of the nucleons.

The Legendre flow equation may be obtained by considering the following integral,

$$
\frac{1}{2} \left(4ix_A\right) \left(4ix_B\right) \left(P_a^\dagger\right)_{kl} \operatorname{Tr}\left(P_a P_b^\dagger\right) \left(P_b\right)_{ij}
$$

$$
\times \int \frac{d^4 k}{(2\pi)^4} F_A(p_i, k) \frac{i}{p_i^0/2 + k^0 - \mathcal{R}\left((\boldsymbol{p}_i/2 + \boldsymbol{k})^2\right) + i\epsilon}
$$

$$
\times \frac{i}{p_i^0/2 - k^0 - \mathcal{R}\left((\boldsymbol{p}_i/2 - \boldsymbol{k})^2\right) + i\epsilon} F_B(k, p_f), \tag{A3}
$$

where we have introduced

$$
\mathcal{R}\left(\boldsymbol{k}^2\right) = \frac{\boldsymbol{k}^2}{2M} - R_\Lambda^{(1)}\left(\boldsymbol{k}^2\right), \tag{A4}
$$

and $1/2$ is the symmetric factor. (Note that the way the IR cutoff functions appear should be taken as symbolic, because it comes from the "naive" inclusion of the cutoff function in the averaged action that however breaks Galilean invariance. A precise, Galilean invariant way is given shortly.)

The problem is that the product of the factors F_A and F_B may be quadratic or higher order in k^0, so that the integral over k^0 appears to diverge. This divergence cannot be regularized by the introduction of the higher order terms in k^0 to the denominator of the propagator, because the results depend on the inverses of (expectedly small) coefficients. It means that the higher order terms drastically change the lower order results, and cannot be accepted.

Note that in the relativistic field theory with dimensional regularization such divergence

32

does not cause a problem, because of analytic continuation.

The divergence comes from the large k^0 region, in other words, from the infinitely short time intervals. But from the EFT point of view, one should have a cutoff on the energies of the intermediate states. (There should be a finite resolution of time.) The cutoff may be of order Λ_0^2/M, where Λ_0 is the physical cutoff on three-momenta. We therefore assume, though implicitly, that k^0 is cutoff at a scale of order Λ_0^2/M and ignore the divergence arising from the k^0 integration. Effectively, it ends up with evaluating the integrand at the (either) pole.

The manipulation of making the cutoff Galilean invariant is evident at the amplitude level: to impose the cutoff on the relative momentum [18]. After doing so, Eq. (A3) becomes

$$\frac{1}{2}\left(4ix_A\right)\left(4ix_B\right)\left(P_a^\dagger\right)_{kl}\mathrm{Tr}\left(P_aP_b^\dagger\right)\left(P_b\right)_{ij}\int\frac{d^3k}{(2\pi)^3}\frac{i\,F_A(p_i,k)F_B(k,p_f)|_{pole}}{A(p_i)-\boldsymbol{k}^2/M+2R_\Lambda^{(1)}(\boldsymbol{k}^2)+i\epsilon},\quad (A5)$$

where we have introduced

$$A(P)\equiv P^0-\frac{\boldsymbol{P}^2}{4M},\quad (A6)$$

and $F_A(p_i,k)F_B(k,p_f)|_{pole}$ denotes that $F_A(p_i,k)F_B(k,p_f)$ is evaluated at the pole.

3.   Equivalence

In order to establish the relation between the Legendre flow equation and the RG equation employed by Birse et al., it is useful to rewrite the Legendre flow equation in the sharp cutoff limit in a simpler form.

In the sharp cutoff limit, the integral in Eq. (A5) may be further simplified, and can be written as

$$-4ix_Ax_B\left(P_a^\dagger\right)_{kl}\left(P_a\right)_{ij}\frac{1}{8\pi^3}\int_\Lambda^\infty k^2dk\int d^2\Omega_k\frac{F_A(p_i,k)F_B(k,p_f)|_{pole}}{A(p_i)-k^2/M+i\epsilon},\quad (A7)$$

where we have used $\mathrm{Tr}\left(P_aP_b\right)=\delta_{ab}/2$. The change of Λ may be compensated by the change of the coupling constants. Thus, if $C_C\sim x_C/\Lambda^{d_C}$,

$$\frac{dx_C}{dt}F_C(p_f,p_i)+d_Cx_CF_C(p_f,p_i)\quad (A8)$$

receives the contribution from

$$-x_Ax_B\frac{1}{8\pi^3}\left(-\Lambda\frac{d}{d\Lambda}\right)\int_\Lambda^\infty k^2dk\int d^2\Omega_k\frac{F_A(p_i,k)F_B(k,p_f)|_{pole}}{A(p_i)-k^2/M+i\epsilon}$$

$$=x_Ax_B\frac{M\Lambda}{8\pi^3}\int d^2\Omega_k\frac{F_A(p_i,\Lambda)F_B(\Lambda,p_f)|_{pole}}{1-\tilde{A}(p_i)},\quad (A9)$$

where $\tilde{A}(P) = MA(P)/\Lambda^2$ and $F_A(p_i, \Lambda)F_B(\Lambda, p_f)|_{pole}$ is the simplified expression for $F_A(p_i, k)F_B(k, p_f)|_{pole}$ with the magnitude of k being Λ. In the center-of-mass frame, all the F_A in the $^1S_0$ channel do not depend on angles, so that we obtain

$$\frac{dx_C}{dt} + d_C x_C = \sum_{A,B} x_A x_B \frac{M\Lambda}{2\pi^2} \left.\frac{F_A(p_i, \Lambda)F_B(\Lambda, p_f)|_{pole}}{1 - \tilde{A}(p_i)}\right|_C, \tag{A10}$$

where $|_C$ stands for the operation of taking coefficient of $F_C(p_f, p_i)$ in the expansion of the right hand side. This is a very handy expression for the sharp cutoff limit.

If we identify the "potential" $V(p_f, p_i; \Lambda)$ as

$$V(p_f, p_i; \Lambda) = -\sum_C x_C F_C(p_f, p_i), \tag{A11}$$

we have

$$\frac{\partial V}{\partial \Lambda} = -\frac{1}{\Lambda}\sum_C \left(\Lambda\frac{dx_C}{d\Lambda}F_C - d_C x_C F_C\right) = \frac{1}{\Lambda}\sum_C \left(\frac{dx_C}{dt} + d_C x_C\right)F_C. \tag{A12}$$

Substituting Eq. (A10), we have

$$\begin{aligned}
\frac{\partial V}{\partial \Lambda} &= \frac{M}{2\pi^2}\sum_A x_A F_A(p_f, \Lambda)\frac{1}{1 - \tilde{A}(p_i)}\sum_B x_B F_B(\Lambda, p_i) \\
&= \frac{M}{2\pi^2}V(p_f, \Lambda; \Lambda)\frac{\Lambda^2}{\Lambda^2 - MA(p_i)}V(\Lambda, p_i; \Lambda).
\end{aligned} \tag{A13}$$

Since $A(p_i) = p_i^0$ in the center-of-mass frame, it is nothing but the RG equation (2.3) employed by Birse et al. [28].

APPENDIX B: CUTOFF FUNCTION DEPENDENCE OF THE RESULTS

In this section, we briefly show how the results for the $^1S_0$ channel depend on the parameter n in the cutoff function R_Λ in Eq. (2.2). We have derived RG equations for an arbitrary value of n, but the expressions look too complicated that we omit them. In the following, we refer the fixed points/lines/surface as [A], [B], etc., as we defined in Sec. III B.

The primary objective of this study is to justify the use of the sharp cutoff limit, which gives the simplest expressions for the RG equations. It is known that the sharp cutoff leads to bad behaviors in the derivative expansion [36], so that it is important to see how the results behave as we approach to the sharp cutoff limit. In particular, we are concerned

34

TABLE I: The dependence on n of the fixed point [B].

n	location of the fixed point	scaling dimensions
2	$(-1.10326, -0.604674, 0.604674, 0, -1.67004, 0, 1.67004, 1.67004)$	$(-5, -4, -4, -4, -3, -2, -1, 1)$
10	$(-1.02722, -0.524991, 0.524991, 0, -1.40602, 0, 1.40602, 1.40602)$	$(-5, -4, -4, -4, -3, -2, -1, 1)$
10^2	$(-1.00287, -0.502587, 0.502587, 0, -1.34072, 0, 1.34072, 1.34072)$	$(-5, -4, -4, -4, -3, -2, -1, 1)$
10^3	$(-1.00029, -0.50026, 0.50026, 0, -1.33407, 0, 1.33407, 1.33407)$	$(-5, -4, -4, -4, -3, -2, -1, 1)$
10^4	$(-1.00003, -0.500026, 0.500026, 0, -1.33341, 0, 1.33341, 1.33341)$	$(-5, -4, -4, -4, -3, -2, -1, 1)$
∞	$(-1, -\frac{1}{2}, \frac{1}{2}, 0, -\frac{4}{3}, 0, \frac{4}{3}, \frac{4}{3})$	$(-5, -4, -4, -4, -3, -2, -1, 1)$

with the possibility that the sharp cutoff may cause non-analytic, or singular behaviors. We therefore consider the smooth (i.e., differentiable) cutoffs which are very close to the sharp cutoff limit. At any rate, we do not pretend to settle the convergence problem caused by sharp cutoffs in the expansion. We only demonstrate numerically that the use of sharp cutoff does not seem to cause a serious problem in our present case. On the other hand, some authors try to extract the information about the convergence of the derivative expansion by looking at the so-called "scheme (in-)dependence" [29]. From our point of view, the "scheme independence" is a necessary, but not sufficient condition for the convergence. The best we can do is to actually enlarge the space of operators as we are doing in this paper.

The trivial fixed point [A] is always there, and has no n dependence at all. The n dependence of the nontrivial fixed points [B] and [C] is given in Tables I and II. The fixed point [B] is very stable against the variation of n. Even though the location changes slightly, the scaling dimensions do not change at all. The fixed point [C] has a stable limit but it has complex scaling dimensions.

We are not completely sure that the "fixed lines" and the "fixed surface" exist for an arbitrary n, because we are unable to obtain the analytic expressions for them. Numerical study indicates that at least "fixed line" [E] is stable. In Table III, we present the n dependence of a particular point ($u_2 = 0$) on the line and the scaling dimensions at the point.

TABLE II: The dependence on n of the fixed point [C]. ν_i^2 means that scaling dimension ν_i is doubly degenerate.

n	location of the fixed point	scaling dimensions
2	$(-2.03159, 1.46753, 1.27909, 0., -2.64366, 0., 1.78644, -1.84813)$	$(-6.36576, (-5.68288)^2, 5, 3, 1, -1.68288 \pm 2.27988i)$
10	$(-2.27317, 2.69046, 1.2095, 0., -5.60121, 0., 1.3641, -2.62099)$	$(-7.85177, (-6.42588)^2, 5, 3, 1, -2.42588 \pm 3.12036i)$
10^2	$(-2.256, 2.79556, 0.984983, 0., -5.98406, 0., 0.934766, -2.2433)$	$(-7.99819, (-6.49909)^2, 5, 3, 1, -2.49909 \pm 3.20057i)$
10^3	$(-2.25064, 2.79559, 0.957635, 0., -5.99646, 0., 0.888947, -2.19038)$	$(-7.99998, (-6.49999)^2, 5, 3, 1, -2.49999 \pm 3.20155i)$
10^4	$(-2.25006, 2.79547, 0.954855, 0., -5.99738, 0., 0.884356, -2.18494)$	$(-8, (-6.5)^2, 5, 3, 1, -2.5 \pm 3.20156i)$
∞	$(-\frac{9}{4}, \frac{123}{44}, \frac{21}{22}, 0, -\frac{92889}{15488}, 0, \frac{13689}{15488}, -\frac{33831}{15488})$	$(-8, (-13/2)^2, 5, 3, 1, (-5 \pm i\sqrt{41})/2)$

TABLE III: The dependence on n of the fixed point $u_2 = 0$ on the line [E]. ν_i^3 means that scaling dimension ν_i is triply degenerate.

n	location of the fixed point	scaling dimensions
2	$(0, 0, 0, 0, 0, 0, 4.41305, 0)$	$((-5)^3, -3, -1, 0, 2, 5)$
10	$(0, 0, 0, 0, 0, 0, 5.51631, 0)$	$((-5)^3, -3, -1, 0, 2, 5)$
10^2	$(0, 0, 0, 0, 0, 0, 5.07010, 0)$	$((-5)^3, -3, -1, 0, 2, 5)$
10^3	$(0, 0, 0, 0, 0, 0, 5.00719, 0)$	$((-5)^3, -3, -1, 0, 2, 5)$
10^4	$(0, 0, 0, 0, 0, 0, 5.00072, 0)$	$((-5)^3, -3, -1, 0, 2, 5)$
∞	$(0, 0, 0, 0, 0, 0, 5, 0)$	$((-5)^3, -3, -1, 0, 2, 5)$

[1] S. Weinberg, Phys. Lett. **B251**, 288 (1990).

[2] S. Weinberg, Nucl. Phys. **B363**, 3 (1991).

[3] S. Weinberg, Phys. Lett. **B295**, 114 (1992), hep-ph/9209257.

[4] S. R. Beane, P. F. Bedaque, W. C. Haxton, D. R. Phillips, and M. J. Savage, in *At the Frontier of Particle Physics, Handbook of QCD*, edited by M. Shifman (World Scientific, 2000), vol. 1, chap. 3, nucl-th/0008064.

[5] P. F. Bedaque and U. van Kolck, Ann. Rev. Nucl. Part. Sci. **52**, 339 (2002), nucl-th/0203055.

[6] E. Epelbaum, Prog. Part. Nucl. Phys. **57**, 654 (2006), nucl-th/0509032.

[7] D. B. Kaplan, M. J. Savage, and M. B. Wise, Phys. Lett. **B424**, 390 (1998), nucl-th/9801034.

[8] D. B. Kaplan, M. J. Savage, and M. B. Wise, Nucl. Phys. **B534**, 329 (1998), nucl-th/9802075.

[9] A. Manohar and H. Georgi, Nucl. Phys. **B234**, 189 (1984).

[10] D. B. Kaplan, M. J. Savage, and M. B. Wise, Nucl. Phys. **B478**, 629 (1996), nucl-th/9605002.

[11] J. Gegelia, J. Phys. **G25**, 1681 (1999), nucl-th/9805008.

[12] U. van Kolck, Nucl. Phys. **A645**, 273 (1999), nucl-th/9808007.

[13] S. Fleming, T. Mehen, and I. W. Stewart, Nucl. Phys. **A677**, 313 (2000), nucl-th/9911001.

[14] S. R. Beane, P. F. Bedaque, M. J. Savage, and U. van Kolck, Nucl. Phys. **A700**, 377 (2002), nucl-th/0104030.

[15] M. C. Birse, Phys. Rev. **C74**, 014003 (2006), nucl-th/0507077.

[16] A. Nogga, R. G. E. Timmermans, and U. van Kolck, Phys. Rev. **C72**, 054006 (2005), nucl-th/0506005.

[17] E. Epelbaum and U. G. Meissner (2006), nucl-th/0609037.

[18] K. Harada and H. Kubo, Nucl. Phys. **B758**, 304 (2006), nucl-th/0605004.

[19] K. G. Wilson and J. B. Kogut, Phys. Rept. **12**, 75 (1974).

[20] K. G. Wilson, Rev. Mod. Phys. **47**, 773 (1975).

[21] F. J. Wegner and A. Houghton, Phys. Rev. **A8**, 401 (1973).

[22] J. Polchinski, Nucl. Phys. **B231**, 269 (1984).

[23] J. F. Nicoll and T. S. Chang, Phys. Lett. **A62**, 287 (1977).

[24] C. Wetterich, Nucl. Phys. **B352**, 529 (1991).

[25] M. Bonini, M. D'Attanasio, and G. Marchesini, Nucl. Phys. **B409**, 441 (1993), hep-th/9301114.

[26] T. R. Morris, Int. J. Mod. Phys. **A9**, 2411 (1994), hep-ph/9308265.

[27] J. Berges, N. Tetradis, and C. Wetterich, Phys. Rept. **363**, 223 (2002), hep-ph/0005122.

[28] M. C. Birse, J. A. McGovern, and K. G. Richardson, Phys. Lett. **B464**, 169 (1999), hep-ph/9807302.

[29] D. F. Litim, Nucl. Phys. **B631**, 128 (2002), hep-th/0203006.

[30] C. A. Bertulani, H. W. Hammer, and U. van Kolck, Nucl. Phys. **A712**, 37 (2002), nucl-th/0205063.

[31] P. F. Bedaque, H. W. Hammer, and U. van Kolck, Phys. Lett. **B569**, 159 (2003), nucl-th/0304007.

[32] D. B. Kaplan (2005), nucl-th/0510023.

[33] M. C. Birse, Phys. Rev. **C77**, 047001 (2008), 0801.2317.

[34] K. Harada, K. Inoue, and H. Kubo, Phys. Lett. **B636**, 305 (2006), nucl-th/0511020.

[35] A. Margaritis, G. Odor, and A. Patkos, Z. Phys. **C39**, 109 (1988).

[36] T. R. Morris, Phys. Lett. **B334**, 355 (1994), hep-th/9405190.

[37] T. R. Morris and J. F. Tighe, JHEP **08**, 007 (1999), hep-th/9906166.

[38] S. R. McKay, A. N. Berker, and S. Kirkpatrick, Phys. Rev. Lett. **48**, 767 (1982).

[39] T. Koike, T. Hara, and S. Adachi, Phys. Rev. Lett. **74**, 5170 (1995), gr-qc/9503007.

[40] T. Hara, T. Koike, and S. Adachi (1996), gr-qc/9607010.

[41] D. R. Phillips, S. R. Beane, and T. D. Cohen, Annals Phys. **263**, 255 (1998), hep-th/9706070.

[42] W. Schützer and J. Tiomno, Phys. Rev. **83**, 249 (1951).

[43] W. Schützer and J. Tiomno, in *New Research Techniques in Physics* (Brazilian Academy of Science, Rio de Janeiro, Brazil, 1951).

[44] N. G. van Kampen, Phys. Rev. **91**, 1267 (1953).

[45] H. M. Nussenzveig, Phys. Rev. **177**, 1848 (1969).

[46] T. N. Pham and T. N. Truong, Phys. Rev. **D31**, 3027 (1985).

[47] B. Ananthanarayan, D. Toublan, and G. Wanders, Phys. Rev. **D51**, 1093 (1995), hep-ph/9410302.

[48] A. Adams, N. Arkani-Hamed, S. Dubovsky, A. Nicolis, and R. Rattazzi, JHEP **10**, 014 (2006), hep-th/0602178.

[49] J. Distler, B. Grinstein, R. A. Porto, and I. Z. Rothstein, Phys. Rev. Lett. **98**, 041601 (2007), hep-ph/0604255.

[50] A. V. Manohar and V. Mateu, Phys. Rev. **D77**, 094019 (2008), 0801.3222.

[51] A. Adams, A. Jenkins, and D. O'Connell (2008), 0802.4081.

[52] D. R. Phillips, S. R. Beane, and M. C. Birse, J. Phys. **A32**, 3397 (1999), hep-th/9810049.

[53] C. A. Regal, C. Ticknor, J. L. Bohn, and D. S. Jin, Phys. Rev. Lett. **90**, 053201 (2003).

[54] J. Zhang, E. G. M. van Kempen, T. Bourdel, L. Khaykovich, J. Cubizolles, F. Chevy, M. Teichmann, L. Tarruell, S. J. J. M. F. Kokkelmans, and C. Salomon, Phys. Rev. **A70**, 030702 (2004).

[55] C. H. Schunck, M. W. Zwierlein, C. A. Stan, S. M. F. Raupach, W. Ketterle, A. Simoni, E. Tiesinga, C. J. Williams, and P. S. Julienne (2004), cond-mat/0407373.

[56] M. C. Birse, private communication. We thank him for explaining his way of getting this fixed point and the scaling dimensions of the perturbations around it.